

A High-Resolution, US-scale Digital Similar of Interacting Livestock, Wild Birds, and Human Ecosystems with Applications to Multi-host Epidemic Spread

Abhijin Adiga^{*1,4}, Ayush Chopra^{*2}, Mandy L. Wilson¹, S. S. Ravi¹, Dawen Xie¹, Samarth Swarup¹, Bryan Lewis¹, Ramesh Raskar² and Madhav V. Marathe^{1,3,4}

¹Biocomplexity Institute, University of Virginia, Charlottesville, VA

²MIT Media Lab, Massachusetts Institute of Technology, Cambridge, MA

³Dept. of Computer Science, University of Virginia, Charlottesville, VA

⁴email: abhijin@virginia.edu and marathe@virginia.edu

Abstract

One Health issues, such as the spread of highly pathogenic avian influenza (HPAI), present significant challenges at the intersection of human, animal, and environmental health. Recent H5N1 outbreaks underscore the need for comprehensive modeling that capture the complex interactions between various entities in these interconnected ecosystems, encompassing livestock, wild birds, and human populations. To support such efforts, we present a synthetic spatiotemporal gridded dataset for the contiguous United States, referred to as a *digital similar*. The methodology for constructing this digital similar involves fusing diverse datasets using statistical and optimization techniques. The livestock component includes farm-level representations of multiple livestock types—cattle, poultry, hogs, and sheep—including further categorization into subtypes, such as milk and beef cows, chicken, turkeys, ducks, etc. It also includes location-level data for livestock-product processing centers. Weekly abundance data for key wild bird species involved in avian flu transmission are included along with temporal networks of movements. Gridded distributions of the human population, along with demographic and occupational features, capture the placement of agricultural workers and the general population. The digital similar is verified and validated in multiple ways. This dataset aims to provide a comprehensive basis for modeling complex phenomena at the wild-domestic-human interfaces.

1 Introduction

Importance and Challenges of High-Resolution Spatiotemporal Modeling. Recent years have seen the development of national-scale, realistic in silico representations that capture data on populations, socioeconomic activities, and built infrastructure to study complex phenomena such as epidemiology, emergency response, and food security at fine spatiotemporal resolutions [8, 17, 20, 30, 52, 60]. Here, we refer to such synthetic datasets as *digital similars*, as they have statistical similarity to real data, but differ from “digital twins”, which are intended as precise replicas of real-world systems. These realistic datasets are used for risk assessment and simulation modeling, as evidenced by studies conducted during the COVID-19 pandemic to analyze infectious disease dynamics [1, 2, 16, 22, 31, 33]. The objective of this work is to develop realistic representations of the wild-domestic-human ecosystems, motivated by the emerging threat of highly pathogenic avian influenza (HPAI).

^{*}These authors contributed equally to this work.

The growing threat of avian influenza to health, agriculture, and the environment. Highly pathogenic avian influenza (HPAI) is a major One Health issue [32, 34]. With increases in virulence of HPAs [36], the risk of a potential pandemic increases, as they continue to affect new regions and more animal categories [38, 57]. The recent H5N1 virus clade, 2.3.4.4b, has gained a lot of attention globally due to the loss of wildlife, including seabirds and aquatic mammals across the globe [10, 35, 52, 53, 59]. In the US, spillover events have caused significant negative impacts to the livestock industry, including large-scale outbreaks in poultry and dairy cattle [9, 11, 45, 52]. There have also been several instances of zoonotic transmissions [12, 13, 15] posing a serious pandemic hazard. Therefore, there is an urgent need to understand the dynamics of HPAI spread for effective surveillance and mitigation of its impact on health and food security.

Multi-pathway spread of HPAs. The introduction and long-range spread of HPAI infections have been primarily attributed to migratory birds and the movement of livestock and livestock products [11, 34, 38, 45, 48, 52], though other pathways may facilitate local spread, including cross-species transmission within and between farms. It is also important to model the distribution of livestock populations into farms of various sizes, as concentrated livestock operations not only act as reservoirs, but can also lead to large outbreaks and rapid spread [28]. In this regard, the impact on the poultry population is notable, with multiple outbreaks across the US affecting millions of chickens [5, 14]. Representing the human population is necessary for studying (i) the role of agricultural workers in the spread, (ii) their susceptibility to zoonotic transmissions, and (iii) the introduction of the disease to the rest of the population. It is critical that modeling efforts account for these known key entities and the interactions among them that drive this spread at the appropriate spatial, temporal, and organization scales.

Challenges. However, building digital similars presents various challenges due to data scarcity, as well as the need to fuse diverse datasets that may have been collected across different spatial resolutions. In the context of livestock, synthetic datasets have been developed to represent spatial population distributions and operations [7, 8, 17, 27], especially relevant to studies on highly pathogenic avian influenza (HPAI) spread [32, 52]. Yet, from the perspective of HPAs, these works tend to focus on a limited set of entities and transmission pathways [32, 52].

Summary of our contributions. This work presents a high-resolution multi-layered spatiotemporal representation of the contiguous US, henceforth referred to as the *digital similar* (*DS*), that captures (i) the distribution of livestock populations and operations, (ii) associated food processing center locations, capacities, and functions, (iii) spatiotemporally-varying wild bird abundances for multiple species, and (iv) human populations with demographic features and attributes capturing agricultural employment, as illustrated in Figure 1. We leverage diverse datasets (detailed in Table 1), such as the Census of Agriculture, the Gridded Livestock of the World (GLW) dataset, eBIRD Status and Trends, and locations of livestock-related operations obtained from multiple sources. Our methods involve a combination of optimization techniques, statistical tools, and graph algorithms. We perform rigorous data quality checks with reference to parent data sets and verification & validation studies using independent data sets including known locations of large livestock farms and H5N1 incidence reports.

The livestock layers consist of four main animal types: cattle, poultry, hogs (pigs), and sheep, with fine grid-level data (5 arc minute resolution) on population size as well as farms. We also include subtypes for cattle (beef and milk) and poultry. The wild bird species include the species of high relevance to HPAI transmissions. To the best of our knowledge, this is the first work that models cattle populations at the national scale. Also, our work extends earlier works on hogs and chickens (e.g., [8, 32, 52]) capturing more livestock types and subtypes. This digital similar aims to provide a comprehensive platform for modeling and risk assessment of HPAI-like phenomena at high spatial and temporal resolutions across the contiguous US, thus informing disease surveillance and control efforts.

Livestock	Heads (\approx)	Farms (\approx)
Cattle	86M*	732K*
- Beef	30M	622K
- Milk	9317802	36K

Poultry		
- Layers	388M	240K
- Broilers	1,680M	42K
- Turkeys	97M	23K
18 other subtypes		

Hogs	62M	60K
Sheep	3M	89K

*M is million and K is thousand.

Wild birds:
39 species such as geese, mallards, crows, etc.

Human population:
 \approx 300M with \approx 2M workers in livestock production and processing.

Processing centers:
Poultry: 4978, slaughter: 2,086, and dairy: 188

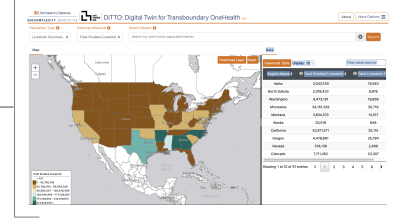
Livestock operations

Processing centers

Wild birds

Human population

Integrating components into a gridded representation



Dashboard

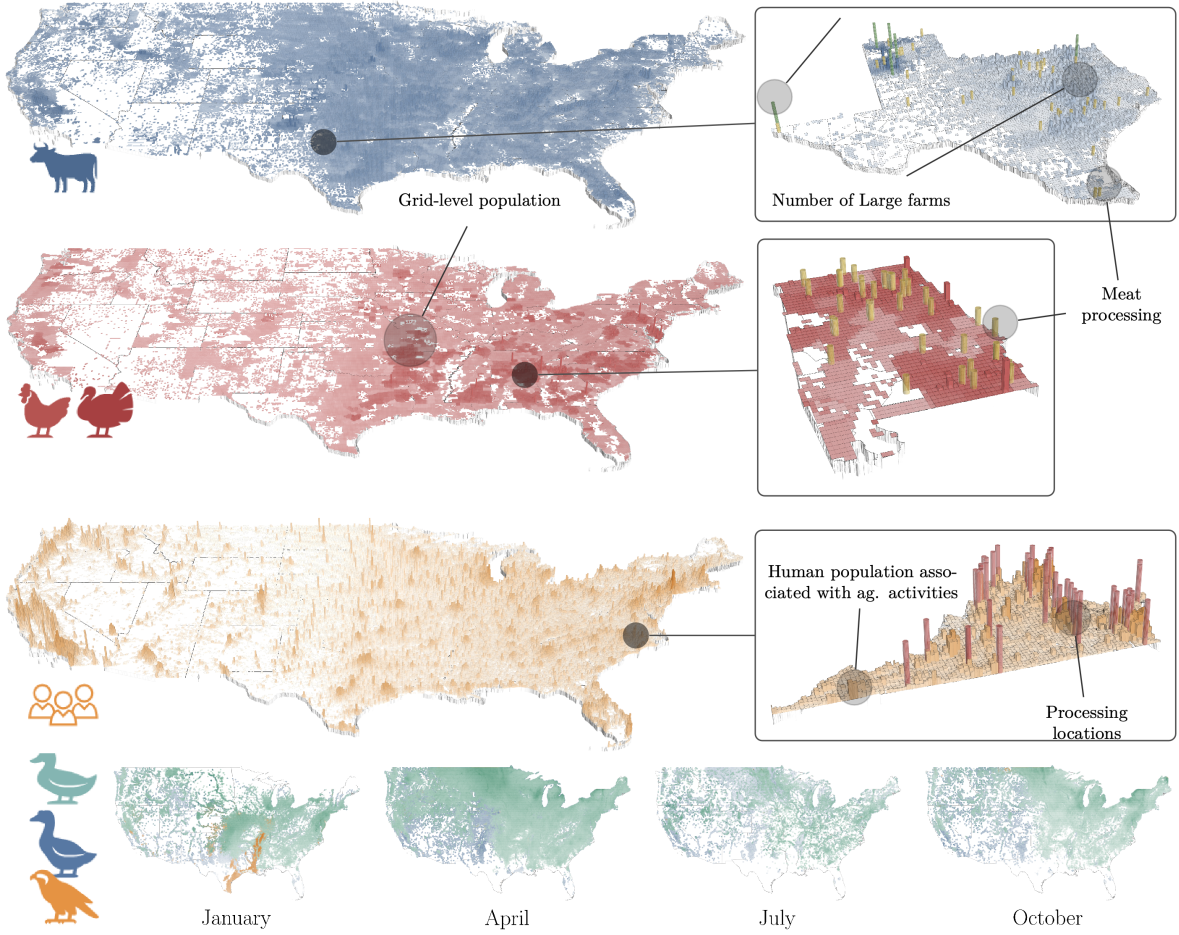


Figure 1: **Overview of the digital similar.** A schematic of the system highlighting the various components including the various entities or agents that are represented, and the dashboard through which the data is exposed is provided at the top. Two of the four livestock layers are shown. We have zoomed in on major production regions for the respective livestock. Both population density and counts of farms are depicted. Also shown are livestock and dairy processing centers. For the human population, agricultural workers are highlighted. The spatiotemporal distribution of three wild birds is shown in the last layer.

2 Results

2.1 The Digital Similar

The digital similar \mathcal{DS} provides a unified gridded representation of livestock production and processing operations, the human population, and wild bird populations in the contiguous US. Figure 1 provides a layered view of the digital similar, and Table 1 (in Section 4) provides an overview of the data sources used to construct it. Formally, $\mathcal{DS}(V, \mathcal{L}, \mathcal{P}, \mathcal{B}, \mathcal{H})$ is defined over a grid V overlaid on the study region, which in our case is the contiguous United States. Each grid cell $v \in V$ has attributes that capture the details of each of these components. In the current setting, we use a 5×5 arc minute² grid that is consistent with Gridded Livestock of the World (GLW) (Table 1), one of the primary data sources that we have used to construct the digital similar. Descriptions of the components \mathcal{L} are provided below.

Livestock $\mathcal{L}(\Theta_{\mathcal{L}}, \{\Gamma_{\theta} \mid \theta \in \Theta_{\mathcal{L}}\}, \{\mathcal{F}_{\theta} \mid \theta \in \Theta_{\mathcal{L}}\})$. The livestock population comprises four types of animals: $\Theta_{\mathcal{L}} = \{\text{cattle}, \text{poultry}, \text{hogs}, \text{sheep}\}$. For each type $\theta \in \Theta_{\mathcal{L}}$, Γ_{θ} denotes the set of different “subtypes” of animals. For example, $\Gamma_{\text{cattle}} = \{\text{beef}, \text{milk}, \text{other}\}$. The full list of subtypes is provided in Figure 1. For each type of livestock, the population is partitioned into farms¹. The collection of farms for each livestock type θ is denoted by \mathcal{F}_{θ} . For each farm $f \in \mathcal{F}_{\theta}$, the population of each subtype γ , denoted by $H_{f\gamma}$, is specified. (We use H for head counts). Also specified is the grid cell v to which this farm is assigned. Note that, in the current digital similar, farms with mixed livestock types (e.g., farms with both cattle and hogs) are not represented. Therefore, the sum total of farms across livestock types would exceed the total number of livestock farms.

Processing centers $\mathcal{P}(\{p\})$. This layer provides locations of livestock-associated food processing centers such as meat processing, dairy processing, and poultry processing units. Each processing unit p contains attributes such as the location of the unit, type of processing, and the size estimate. Appendix C provides details about how we stratify the processing plant likelihood of dealing with unpasteurized milk.

Wild birds $\mathcal{B}(\Theta_{\mathcal{B}}, A(\cdot), G_{\mathcal{B}})$. This component captures the spatiotemporal distribution of multiple species of birds identified as significant vectors of avian influenza based on H5N1 incidence data from 2022–2024. There are 36 species of birds represented in this component derived from EBIRD data and H5N1 incidence data from 2022–2024 (see Table 1 for the data sources). Let $\Theta_{\mathcal{B}}$ denote the set of different species (listed in Figure 1). The abundance of a species $\theta \in \Theta_{\mathcal{B}}$ in grid cell $v \in V$ at time t is denoted by $A(\theta, v, t)$. The data is available at a weekly resolution.

Human population $\mathcal{H}(\Delta, \mathcal{E}, \pi(\cdot))$. This component provides a grid-level representation of the human population with emphasis on agricultural workers (associated with livestock and its processing). For each cell v , $\pi(v, \delta, \epsilon)$ denotes the size of the subpopulation that belongs to the demographic group $\delta \in \Delta$ defined by attributes including age group and sex and employed in professional classes specified by $\epsilon \in \mathcal{E}$. An employment group ϵ is defined by occupation and industry attributes, where non-agricultural employees are all binned into one group, namely non-agriculture.

2.2 Verification, Validation and Data Quality

2.2.1 Livestock

Farm generation and cell assignment. We compared the total head counts from the assigned farms with the corresponding counts from the AGCENSUS data. The aggregation was done at the state level. The absolute relative difference is plotted in Figure 2 (top row). The differences between the modeled head counts and AgCensus are caused by the assignment of head counts to areas where AgCensus head counts were

¹All livestock production operations will be referred to as farms.

unreported, and by subsequent adjustment of counts for consistency across farm sizes (Section A.4). We observe that the relative difference is below 1% in most instances, barring a few outliers. Also, the larger the population of a subtype, the smaller the relative difference. Figure 2 (bottom row) shows the distribution of the livestock population into farms. The largest cattle farms are assigned around 100,000 heads, while chicken farms (corresponding to subtypes layers and broilers) can be assigned up to 3 to 5 million heads.

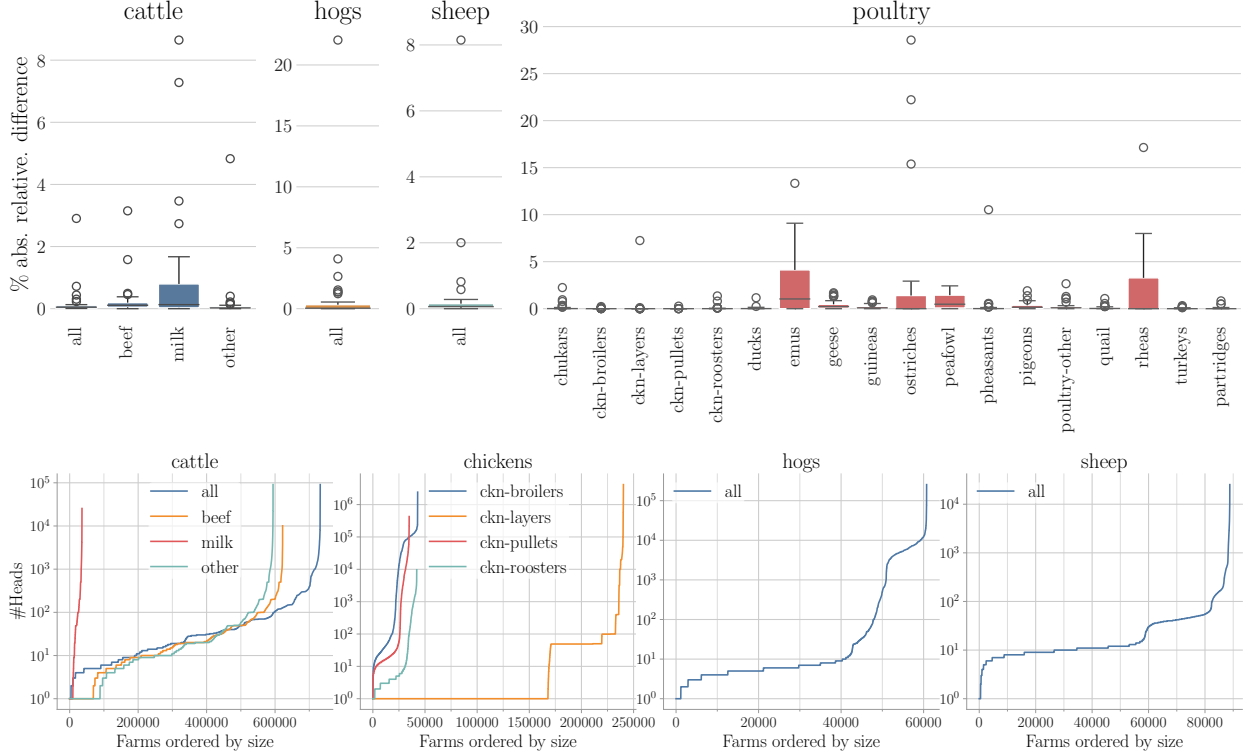


Figure 2: The plots in the first row compare head counts of assigned farms with AGCENSUS state totals. The absolute relative difference between state-level head counts aggregated across farms and the AGCENSUS data is plotted. The second row shows the distribution of livestock populations among farms.

We analyze the performance of Algorithm 2 (GENFARMS). Recall that in this algorithm, the minimization objective includes the parameter λ_1 . This parameter bounds the error in livestock totals by farm size category between the reported value and our assignment. (This error is due to the gap filling step carried out by the IPF process.) Our results in Figure 3(a) show that this discrepancy is low across livestock types; the assignment is close to the known total head counts. We analyze the performance of Algorithm 3 (FARMSTOCELLS) in two ways, evaluating how well the assignment of farms aligns with GLW dataset. In Figure 3(b), we plot the parameter λ_5 (see supplement A4), which corresponds to the maximum absolute difference between the head counts corresponding to our assignment and GLW cells. The second plot in Figure 3(b) measures the alignment using Pearson’s correlation coefficient. For all livestock types except poultry, the correlation is on an average around 0.75. However, there are instances which are negatively correlated with GLW. The reason for this behavior is that larger farm sizes make it more difficult to align the head counts with cell capacities. In general, poultry distribution is weakly correlated with GLW.

Comparing generated farm locations with known operations. Concentrated Agricultural Feed Operations (CAFOs) are large animal feeding operations that are a potential hazard to the environment and the health of individuals in the adjoining communities. We obtained data from CAFOMAPS [47], which

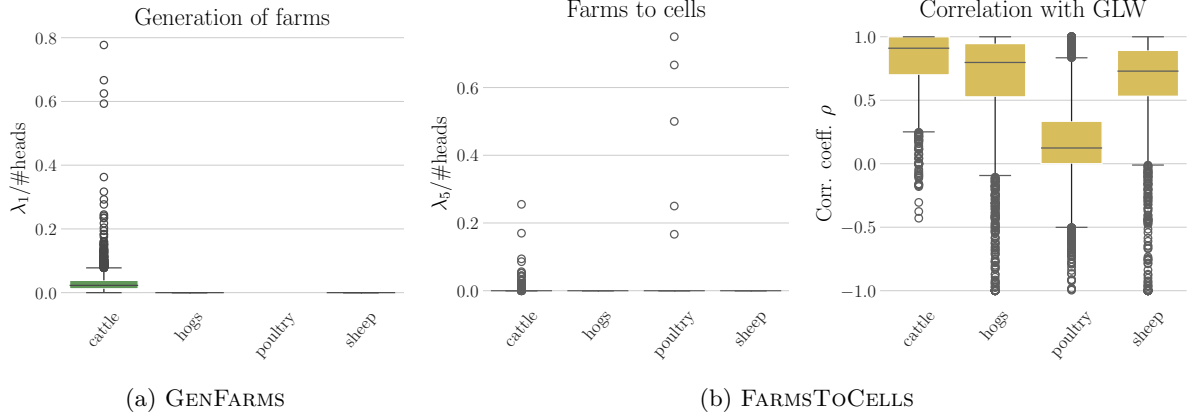


Figure 3: (a) Analysis of GENFARMS algorithm: We plot the value of the parameter λ_1 relative to the number of heads. Lower is better. We also plot this value for a restricted set of instances where the county totals are known. (b) Analysis of FARMSToCELLS algorithm: Both plots indicate the alignment of the farm assignment with GLW data. The first plot corresponds to parameter λ_4 for county–livestock instances relative to the number of heads; lower is better. Using the Pearson correlation coefficient, cell-level head counts aggregated from our farm assignment are compared with GLW head counts; higher is better.

provides the physical locations of several CAFOs. We focus on cattle, hogs, and chickens. For each county–livestock instance for which such data is present, we selected large farms from our farm assignment based on livestock-specific thresholds informed by CAFO size specifications provided by various states [51]. We computed the Haversine distance of each CAFO location to the centroid of each grid cell that contains a large farm. We construct a weighted complete bipartite graph $G(A, B)$ for each county–livestock instance. Here A corresponds to farm locations from our assignments; each farm is assumed to be located at the centroid of the grid cell to which it belongs. The set B corresponds to CAFO locations. For each $u \in A$ and $v \in B$, the weight on the edge (u, v) is the inverse of the distance between the two locations. We compute a maximum weighted perfect matching² of this bipartite graph to match each CAFO location to a farm in \mathcal{DS} . The main objective is to map as many CAFO locations as possible. It is possible that the number of farms is greater than the number of CAFO locations as not all locations are listed. The results of the matching are analyzed in Figure 4. We considered two sets of thresholds, the second set corresponding to larger farms compared to the first. A large percentage of CAFO locations were matched in the case of cattle ($> 95\%$) and chickens ($> 83\%$), while in the case of hogs we observe only 50% match. A closer examination of AGCENSUS data reveals the reason for the low number of matches for hogs: the number of farms specified by the parent dataset for the relevant size categories is less than the number of CAFO locations specified. Among the matched locations, we observe that 90% of the CAFO locations are at most 10 miles from the grid centroid of the corresponding farm from the digital similar, which places it in the same grid cell or a neighboring one. We note that a majority of matched CAFO farms corresponding to cattle and hogs are within 20 miles of the matched farm in \mathcal{DS} .

2.2.2 Wild birds

Bird abundance and H5N1 incidence. We compare the relative abundance of the chosen bird species, as captured in the \mathcal{DS} , with the occurrence of H5N1 cases at state level. We recall that we chose to include all the species with reference to H5N1 incidence data from 2022–2024. The objective is to ascertain whether there are H5N1 incidences among the most abundant birds in each state where cases have been reported. This is relevant to colocation-based risk analysis that is discussed later where bird abundance influences the risk estimates. For each state, we calculated the average abundance for each bird species over the study

²For a complete bipartite graph $G(A, B, E)$, where $|A| = m$ and $|B| = n$, a perfect matching consists of $\min\{m, n\}$ edges.

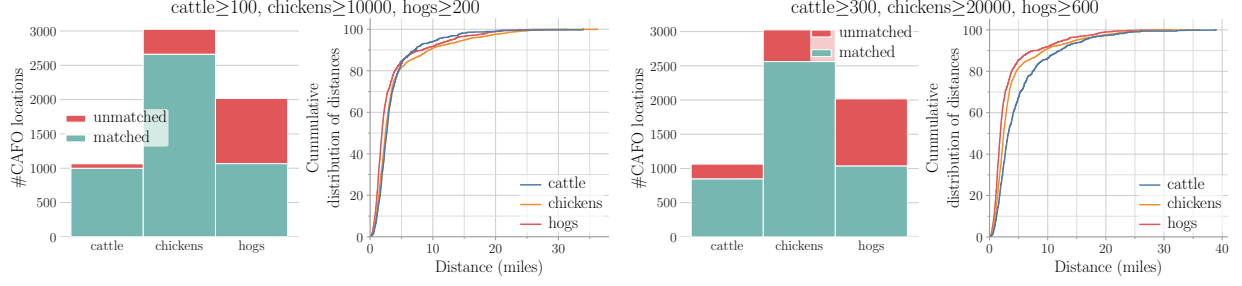


Figure 4: Analysis of mapping CAFO locations by livestock type to farms from the digital similar. The two plots correspond to two sets of thresholds for choosing the farms to compare with. The second set corresponds to larger farms compared to the first. In each plot, the first subplot shows how many CAFO locations were matched. The second subplot provides the cumulative distribution of the distances (in miles) between matched pairs of CAFO locations and farms.

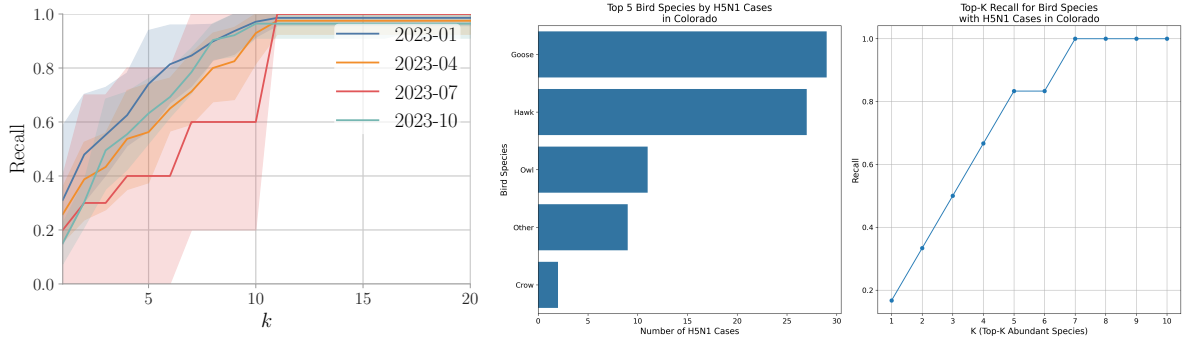


Figure 5: Analysis of H5N1 cases and bird abundance for the period of January to December of 2023. The plot on the left summarizes the results across states for the four quarters. The plot on the right orders the top five abundant birds by population and shows the H5N1 incidences for the state of Colorado.

period (January 1 to March 30, 2023) breaking down the period in to four quarters. We then compiled H5N1 case counts for each bird species in the same state and time frame. Bird species were grouped into 15 categories (e.g., ‘Duck’, ‘Goose’, ‘Eagle’) to account for variations in species naming and to provide more robust comparisons. We employed **top-K recall** metric to quantify the relationship between bird abundance and H5N1 cases. It is the proportion of species with H5N1 cases that are among the K most abundant species in a state within the target period and administrative region.

$$\text{Top-K Recall} = \frac{\text{Species with H5N1 cases in top-K abundant species}}{\text{Total species with H5N1 cases}}.$$

The results are presented in Figure 5. The plot on the left summarizes the Top-K recall results for all states and different parts of the year. We observe that for all quarters, the larger the bird population, the greater the likelihood of observed H5N1 cases. Secondly, we observe that in most cases, the top 10 abundant birds cover all H5N1 cases (for $k \geq 10$), the recall value is close to 1. The plot on the right shows the results for Colorado, which is at the epicenter of the large number of recent outbreaks [46]. These results suggest a robust correlation between bird abundance and H5N1 case occurrences.

3 Discussion

Related work. Several models have been proposed for subcounty-level disaggregation of livestock population. Using a random forest model, Gilbert et al. [27] develop a global distribution of populations of multiple livestock types. Burdett et al. [8] develop the FLAPS model to simulate populations and locations of individual farms for swine using the AGCENSUS dataset and a microsimulation model. This work was used in the analysis of the spread of porcine deltacoronavirus in the US [49]. Our work utilizes the IPF-based methodology proposed by Burdett et al. to fill gaps in livestock types and subtypes. Cheng et al. [17] develop the MAPS model to map swine production in China using enterprise registration information and other datasets. For mapping concentrated animal feeding operations (CAFOs), several deep learning methods have been proposed to map industrial operations using remote sensing data [29, 54]. In the context of HPAs, there is a need for significant extensions to these works given the requirement to simultaneously account for multiple livestock types and wild birds, as well as organizational-level distributions. In a very recent work, Prosser et al. [52] address estimation of transmission risk at the wild waterfowl–domestic poultry interface. They develop a spatiotemporal model combining 10 species-level wild bird abundance models [56] with a commodity-level poultry farm model [50]. They perform phylogenetic analyses to identify wild bird spillover events to validate their model at two spatial scales, namely grid-level and county-level. Humphreys et al. [32] use a variety of datasets including GLW to model waterfowl movement and interactions with poultry farms and human population. The authors apply Bayesian joint hierarchical modeling to model species distributions as a function of time and migration timing.

Limitations. While this dataset offers valuable insights as demonstrated in our work, it is important to acknowledge its limitations and potential for future improvements. The dataset faces challenges primarily stemming from the nature of parent datasets. For example, the synthetic dataset GLW is misaligned in time with respect to AGCENSUS. In addition, as shown in our analysis with respect to operations whose locations are known, not all assigned operations are matched indicating spatiotemporal misalignment with AGCENSUS. Unlike some previous works [8, 52], we do not produce coordinate-level assignments for operations. While this might become a limitation for very fine-grained analysis such as farm-to-farm movement of animals, for such datasets to be useful, additional location- and operation-level information and rigorous validation is required. Another important limitation of our work is that it does not model mixtures of different livestock types (such as cattle and poultry in the same farm). Some livestock types (like poultry) do not have adequate farm size information, leading to heavy-tailed distribution of populations across farms. While the current openly available AGCENSUS data does not provide this data, further exploration of cross-tabulation data that is available by request could allow us to improve on these aspects. In those instances where even state and county totals are absent, we fill gaps based on an equitable distribution of the missing heads (details in Methods). This might not represent ground truth. For wild birds, EBIRD status and trends data provides only relative abundance measures, which are subject to observational biases and tend to underestimate true populations. Further, our gravity model for the migration network does not consider historical migration trajectories and may oversimplify complex movement patterns. The approaches used in BirdFlow [26] require more data on trajectories. Finally, mapping agricultural workers to farms is a challenging task as it is a function of farm size, livestock type, and the level of automation employed [39]. Also, our data does not explicitly account for non-immigrant temporary workers as they are not adequately captured by the US Census. Capturing pathways of spread requires modeling movements of animals (within and between farms, as well as inter-state movement), role of human beings, more precise interactions with wildlife, etc. Despite these limitations, our dataset provides a valuable foundation for studying complex interactions between livestock, wild birds, and human populations in the context of avian influenza transmission.

Conclusion. Our work presents a comprehensive methodology to construct synthetic spatiotemporal datasets of food systems, human population, and wildlife, with emphasis on the spread of HPAI-like diseases. Beyond the study of H5N1, the dataset offers valuable applications to other One Health issues and beyond. The modular nature of the digital similar enables us to leverage subsets of layers depending on the nature

of the application. This dataset can be applied to model the spread of other pathogens, such as West Nile virus or Salmonella, which also involve interactions between livestock and human populations [37, 42, 61]. Such systems have value beyond infectious diseases in domains such as food safety, agricultural economics, environmental damage, pollution, disaster response, biosecurity, and supply chain problems [8, 27, 47, 63]. In biodiversity and conservation efforts, the wildbird abundance data can aid in identifying critical habitats and migration corridors, particularly in the context of livestock operations. Spatially explicit synthetic datasets are being extensively developed for such non-epidemiological settings [6, 40, 41, 58, 62]. Our digital similar can extend such works to account for additional ecosystems such as livestock in the respective applications.

4 Methods

4.1 Datasets

Table 1 summarizes all data used. We used publicly available datasets, which can be categorized into three types: census, synthetic realistic datasets derived from models and data samples, and real location-level datasets. From a spatial unit perspective, some data (e.g., AGCENSUS and H5N1 incidence data) are specified at various administration levels, some data (e.g., GLW and EBIRD) are specified at grid-level, while for the rest, exact locations are provided. Some of these datasets have been used for the construction of the digital similar while the rest have been used for subsequent analysis. More details about each dataset are provided in the relevant sections.

Table 1: Datasets explored to construct the digital twin.

Name	Abbrev.	Source	Description
Census of Agriculture	AGCENSUS	[19, 43, 44]	Provides location-level Ag data, such as number of farms, farm sizes, crop types, and fallowed status. Provides individual-level Ag data such as the number of workers in a farm.
Gridded Livestock of the World	GLW	[21, 27, 55]	GLW4.0 provides distribution maps for several livestock. FAO hosts this website.
eBird Status and Trends	EBIRD	[24, 56]	Weekly data of relative abundance of migratory birds across geospatial regions throughout the year.
Dairy processing	Dairy plants	[3]	Large dairy processing centers and their attributes.
Meat, poultry, and egg processing	Meat and poultry	[25]	Listing of establishments that produce meat, poultry, and/or egg products regulated by FSIS.
CAFOs in the US	CAFOMAPS	[47, 51]	A map of Concentrated Animal Feeding Operations (CAFOs) in the Southern United States covering nine states.
H5N1 outbreak by APHIS	H5N1CASES	[4]	H5N1 bird flu detections in wild birds, livestock, and humans by state and county

4.2 Livestock

Here, we provide an overview of the process of generating the livestock layers. Additional details appear in the supplement. The types of livestock covered in this work are summarized in Figure 1. Two data sources were used to construct the livestock layers: Census of Agriculture (AGCENSUS) and Gridded Livestock of the

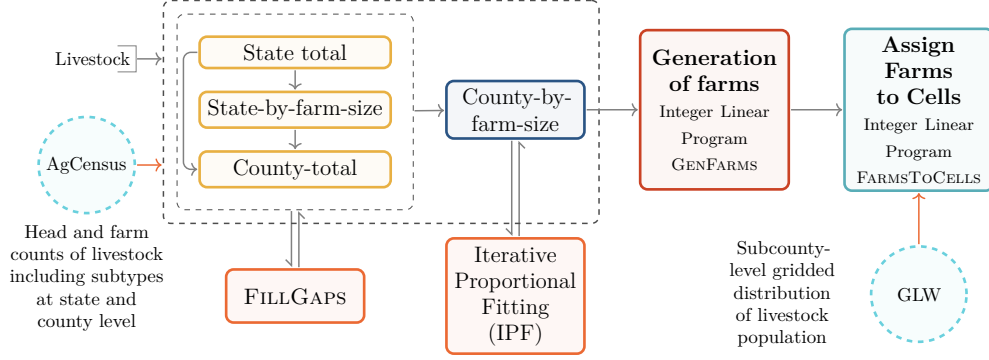


Figure 6: A schematic of the livestock layer construction, including data processing, generation of farms and assignment of cells to farms.

World (GLW). These are described in the following sections. An overview of the methodology is provided in Figure 6. We recall the definitions of livestock type and subtype from the model description in Section 2.1.

Data organization and availability challenges. AGCENSUS provides counts of heads (i.e., population size) and farms for various livestock types and subtypes. The data is available at three different administrative levels – country, state, and county. The data organization is livestock type specific, making it a non-trivial task to extract relevant information. Farms are binned into categories based on the head counts of the corresponding livestock type. We preprocessed the data to ensure that these categories are disjoint and the categorization is identical at both state and county levels. Ideally, given a livestock subtype and administrative level, both farm and head counts are provided for each farm size category. Also provided is the total count of farms and heads. Together, we have four possible types of counts: (i) state-total: total number of farms/heads, (ii) state-by-farm-size: number of farms/heads per farm size category, and corresponding county-level counts (iii) county-total and (iv) county-by-farm-size. More details with examples are provided in the supplement. However, some head counts are missing in all count types. In the case of poultry, even farm size categories are missing for all subtypes except for layers. The Gridded Livestock of the World [21] dataset provides a gridded distribution of livestock abundance at 5 arc minute resolution. The details of the processing of GLW are provided in the supplement.

Filling gaps in data. We use a combination of integer linear programs (ILPs) and iterative proportional fitting (IPF), the latter, following Burdett et al. [8]. For cattle and poultry, gaps are filled for each subtype, while for hogs and sheep, they are filled for the livestock type. We use the integer program Algorithm 1 (described in the supplement) to fill missing data for the following types of counts: state-total, state-by-farm-size, and county-total. It takes as input all the known counts, sum of all the counts, and bounds on the unknown counts and distributes equitably the heads that are unaccounted for to all entities for which the counts are missing. It respects the bounds provided as input. To fill gaps in county-by-farm-size counts, we follow the methodology of Burdett et al. [8]. They apply IPF [18, 23] for the case of hogs to estimate these counts. At each step, the objective is to make use of all the available data (in all count types). Since subtypes are processed independently, the resulting counts can lead to infeasible instances. The farm generation ILP (described later) handles such cases.

Farms to cells. Here, given a livestock type and county, the objective is to obtain a grid-level distribution of farms that is consistent with the AGCENSUS data from the perspective of operations and their sizes and the GLW data from the perspective of the grid-level distribution of livestock population. We use a two-step procedure using optimization algorithms: (i) generating farms consistent with the county-by-farm-size counts (either provided for or estimated) and (ii) assigning farms to cells. The GENFARMS algorithm for generating

farms is described in the supplement. The objective function encodes several minimization criteria. They are stated in the order of priority: (i) Feasibility: modifies the subtype head count minimally to ensure feasibility of the assignment (ii) Equitable distribution of head counts for each subtype of livestock across farms within a category, (iii) Minimize the number of subtypes within a farm, and (iv) align with known county-by-farm-size counts. The FARMSTOCELLS algorithm assigns a cell to each farm. The objective of this algorithm is to ensure that the head counts resulting from the assignment and GLW head counts are as closely aligned as possible.

4.3 Wild Bird Abundance and Movement

We leveraged data from eBird’s Status and Trends products [24] (see EBIRD in Table 1) to construct this component. We recall that this component $\mathcal{B}(\Theta_{\mathcal{B}}, A(\cdot), G_{\mathcal{B}})$ captures spatiotemporal abundance and movement of multiple species of birds. The EBIRD (Table 1) data provides weekly estimates of relative bird abundance across a high-resolution grid (2.96km \times 2.96km). These estimates, derived from ensemble machine learning models, represent the expected count of a species on a standardized eBird checklist at a given location and date. The models combine millions of citizen science observations with environmental predictors, accounting for factors such as land cover, climate variables, and observation effort. A relative abundance of 1.0 for a species at a particular location and time would indicate that an average eBird checklist at that place and time would be expected to count one individual of that species. Higher values indicate more individuals would be expected, while lower values indicate the species would be observed less frequently or in smaller numbers. This approach ensures that our model captures the most relevant species for studying avian influenza transmission. We chose bird species for which H5N1 cases were observed in the period 2022-2024. A total of 40 birds were identified of which abundance data was available for 36 species. For each of the selected species, we extract relative abundance values along with their associated geographic coordinates for all 52 weeks in the year. Our processing pipeline is described in the supplement.

4.4 Dairy, Meat, and Egg Processing Plants

We provide a layer of animal product processing plants with attributes such as size, type of processing (dairy, meat, egg, etc.), livestock type, etc. (see Table 1). We use data from Agricultural Marketing Services [3] for a list of large dairy processing plants. These facilities process diverse categories of dairy products, ranging from fluid milk and cream to various types of cheese, butter, and specialty products identified by product codes. We have developed a classification of dairy plant codes based on the likelihood of handling unpasteurized milk. This likelihood can help in spillover risk assessment as well as inform surveillance strategies to detect HPAI incidences (through, for e.g., bulk testing) in associated dairy farms. This classification, is presented in a table in the supplement, categorizing product codes into high, medium, and low-risk groups. We extract data from Food Safety and Inspection Service (USDA) which maintain a comprehensive list of meat and egg processing establishments that need permits to be operational. The data is updated weekly. For these plants, attributes such as size, address, plant type (poultry or slaughter), and coordinates are available. Data from both sources were combined and standardized to form this layer.

4.5 Human Population

We develop a gridded representation of the US population with rich demographic and employment related attributes. This data is derived from a synthetic digital twin [20, 30] that is developed using diverse datasets such as census data, land use data, activity patterns, building maps, etc. Each individual in the population is associated with occupation, identified by the Standard Occupational Classification code (SOCP) and industry, identified by the North American Industry Classification System (NAICS) code. We identified all occupational and industry codes that include livestock employment. These are listed in the supplement. Individuals whose SOCP or NAICS codes did not belong to this list were assigned a default code 0. For each combination of demographic attributes δ and employment ϵ , the population is aggregated at the grid cell

level. Our estimates of livestock worker counts are consistent with the American Community Survey, when aggregated to the US Census Public Use Microdata Area (PUMA) level.

5 Usage Notes

5.1 Visualizations and Access

The synthetic spatiotemporal dataset of interacting livestock and wild bird populations is designed to be easily accessible to and usable by researchers, policymakers, and modelers interested in studying avian influenza dynamics. We provide an interactive visualization dashboard, Digital Twin for Transboundary OneHealth (DiTTO) (shown in Figure 7) to make the data available.

The dashboard user interface is divided into three sections: a navigation bar, where users can indicate which data layers they are interested in viewing, including by population type, relevant subtypes (under Heatmap Measure), and even to pinpoint specific regions. On the lower left side of the screen is a heatmap where users can view where the selected population type is prevalent; users can view that data at US state resolutions, or drill down to view county resolution heatmaps for the selected state. On the lower right side of the user interface is a data table where users can view the actual counts across all of the subtypes for the selected population type and region(s). Users can download the datasets in two ways from the web portal: (i) they can click on the Download Table button above the data table to download the queried rows displayed in the data table, or they can click on the Download Layer button on the map to download the complete grid-level layer data for the selected population type.

In short, DiTTO provides the following key features to make the datasets accessible to its users.

- Interactive maps showing the distribution of livestock, farms, wild bird populations, human populations, and processing centers at the state and county levels.
- The ability to search for specific regions for easier comparison
- Filters for selecting specific regions, time periods (for wild birds), and livestock types.
- Download functionality for either the complete layer or for a subselection of that layer.

References

- [1] Matthew Abueg, Robert Hinch, Neo Wu, Luyang Liu, William Probert, Austin Wu, Paul Eastham, Yusef Shafi, Matt Rosencrantz, Michael Dikovsky, et al. Modeling the Combined Effect of Digital Exposure Notification and Non-Pharmaceutical Interventions on the COVID-19 Epidemic in Washington State. *MedRxiv*, pages 2020–08, 2020.
- [2] Alberto Aleta, David Martin-Corral, Ana Pastore y Piontti, Marco Ajelli, Maria Litvinova, Matteo Chinazzi, Natalie E Dean, M Elizabeth Halloran, Ira M Longini Jr, Stefano Merler, et al. Modelling the Impact of Testing, Contact Tracing and Household Quarantine on Second Waves of COVID-19. *Nature Human Behaviour*, 4(9):964–971, September 2020.
- [3] USDA AMS. Dairy plants surveyed and approved for usda grading service. <https://apps.ams.usda.gov/dairy/ApprovedPlantList/>, 2024. [Accessed 08-2024].
- [4] APHIS. USDA reported H5N1 bird flu detections in US wild birds. <https://www.aphis.usda.gov/livestock-poultry-disease/avian/avian-influenza/hpai-detections>. [Accessed 23-08-2024].
- [5] USDA APHIS. Confirmations of Highly Pathogenic Avian Influenza in Commercial and Backyard Flocks. <https://www.aphis.usda.gov/livestock-poultry-disease/avian/avian-influenza/hpai-detections/commercial-backyard-flocks>, 2023. [Accessed 28-08-2024].
- [6] Christopher Barrett, Keith Bisset, Shridhar Chandan, Jiangzhuo Chen, Youngyun Chungbaek, Stephen Eubank, Yaman Evrenosoğlu, Bryan Lewis, Kristian Lum, Achla Marathe, et al. Planning and response

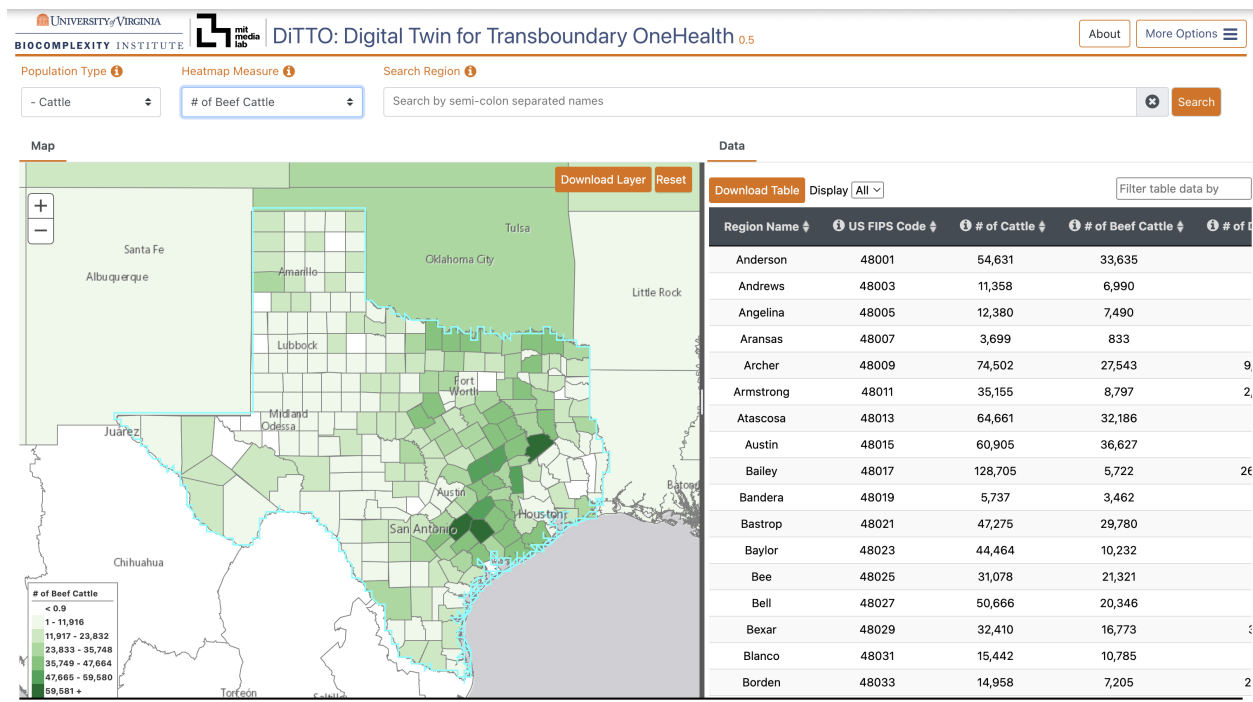


Figure 7: The interactive visualization dashboard allows users to explore the livestock and avian populations in an interactive, spatiotemporal way. It is available at <https://ditto.bii.virginia.edu>.

in the aftermath of a large crisis: An agent-based informatics framework. In *2013 Winter Simulations Conference (WSC)*, pages 1515–1526. IEEE, 2013.

- [7] Mark C Bruhn, Breda Munoz, James Cajka, Gary Smith, Ross J Curry, Diane K Wagener, and William D Wheaton. Synthesized population databases: a geospatial database of us poultry farms. *Methods report (RTI Press)*, page 1, 2012.
- [8] Christopher L Burdett, Brian R Kraus, Sarah J Garza, Ryan S Miller, and Kathe E Bjork. Simulating the distribution of individual livestock farms and their populations in the United States: An example using domestic swine (*Sus scrofa domestica*) farms. *PloS one*, 10(11):e0140338, 2015.
- [9] Eric R Burrough, Drew R Magstadt, Barbara Petersen, Simon J Timmermans, Phillip C Gauger, Jianqiang Zhang, Chris Siepker, Marta Mainenti, Ganwu Li, Alexis C Thompson, et al. Highly pathogenic avian influenza A (H5N1) clade 2.3. 4.4 b virus infection in domestic dairy cattle and cats, United States, 2024. *Emerging infectious diseases*, 30(7):1335, 2024.
- [10] Valentina Caliendo, NS Lewis, A Pohlmann, SR Baillie, AC Banyard, Martin Beer, IH Brown, RAM Fouchier, RDE Hansen, TK Lameris, et al. Transatlantic spread of highly pathogenic avian influenza H5N1 by wild birds from Europe to North America in 2021. *Scientific reports*, 12(1):11729, 2022.
- [11] Leonardo C Caserta, Elisha A Frye, Salman L Butt, Melissa Laverack, Mohammed Nooruzzaman, Lina M Covaleta, Alexis C Thompson, Melanie Prarat Koscielny, Brittany Cronk, Ashley Johnson, et al. Spillover of highly pathogenic avian influenza h5n1 virus to dairy cattle. *Nature*, pages 1–8, 2024.
- [12] CDC. CDC confirms human cases of H5 bird flu among Colorado poultry workers. <https://www.cdc.gov/media/releases/2024/p-0715-confirm-h5.html>. [Accessed 08-21-2024].

- [13] CDC. CDC Confirms Human H5 Bird Flu Case in Missouri. <https://www.cdc.gov/media/releases/2024/s0906-birdflu-case-missouri.html>. [Accessed 10-13-2024].
- [14] CDC. H5 Bird Flu: Current Situation. <https://www.cdc.gov/bird-flu/situation-summary/index.html>. [Accessed 23-08-2024].
- [15] CDC. Highly Pathogenic Avian Influenza A (H5N1) virus infection reported in a person in the U.S. <https://www.cdc.gov/media/releases/2024/p0401-avian-flu.html>. [Accessed 08-21-2024].
- [16] Jiangzhuo Chen, Stefan Hoops, Achla Marathe, Henning Mortveit, Bryan Lewis, Srinivasan Venkatramanan, Arash Haddadan, Parantapa Bhattacharya, Abhijin Adiga, Anil Vullikanti, et al. Effective Social Network-Based Allocation of COVID-19 Vaccines. *Proceedings of the KDD Health Day*, 2022.
- [17] Mingjin Cheng, Xin Liu, Hu Sheng, and Zengwei Yuan. MAPS: A new model using data fusion to enhance the accuracy of high-resolution mapping for livestock production systems. *One Earth*, 6(9):1190–1201, 2023.
- [18] W. Edwards Deming and Frederick F. Stephan. On a least squares adjustment of a sampled frequency table when the expected marginal totals are known. *The Annals of Mathematical Statistics*, 11(4):427–444, 1940.
- [19] ESRI. USDA Census of Agriculture 2017 - cattle production. <https://www.arcgis.com/home/item.html?id=53137233a760432bb07c417eb3d758b8>. [Accessed 06-03-2024].
- [20] Stephen Eubank, Hasan Guclu, VS Anil Kumar, Madhav V Marathe, Aravind Srinivasan, Zoltan Toroczkai, and Nan Wang. Modelling Disease Outbreaks in Realistic Urban Social Networks. *Nature*, 429(6988):180–184, 2004.
- [21] FAO. GLW 4: Gridded Livestock Density. <https://data.apps.fao.org/catalog/dataset/15f8c56c-5499-45d5-bd89-59ef6c026704>. [Accessed 06-03-2024].
- [22] Luca Ferretti, Chris Wymant, Michelle Kendall, Lele Zhao, Anel Nurtay, Lucie Abeler-Dörner, Michael Parker, David Bonsall, and Christophe Fraser. Quantifying SARS-CoV-2 Transmission Suggests Epidemic Control with Digital Contact Tracing. *Science*, 368(6491):eabb6936, 2020.
- [23] Stephen E. Fienberg. An iterative procedure for estimation in contingency tables. *The Annals of Mathematical Statistics*, 41(3):907–917, 1970.
- [24] Daniel Fink, Tom Auer, Alison Johnston, Matt Strimas-Mackey, Shawn Ligocki, Orin Robinson, Wesley Hochachka, Lauren Jaromczyk, Cynthia Crowlye, Kylee Dunham, Andrew Stillman, Ian Davies, Amanda Rodewald, Viviana Ruiz-Gutierrez, and Chris Wood. eBird status and trends, data version: 2022; released: 2023, 2023.
- [25] USDA FSIS. Meat, poultry and egg product inspection directory. <https://www.fsis.usda.gov/inspection/establishments/meat-poultry-and-egg-product-inspection-directory>, 2024. [Accessed 08-2024].
- [26] Miguel Fuentes, Benjamin M Van Doren, Daniel Fink, and Daniel Sheldon. Birdflow: Learning seasonal bird movements from ebird data. *Methods in Ecology and Evolution*, 14(3):923–938, 2023.
- [27] Marius Gilbert, Gaëlle Nicolas, Giusepina Cinardi, Thomas P Van Boeckel, Sophie O Vanwambeke, GR Wint, and Timothy P Robinson. Global distribution data for cattle, buffaloes, horses, sheep, goats, pigs, chickens and ducks in 2010. *Scientific data*, 5(1):1–11, 2018.
- [28] Michael Greger. The human/animal interface: emergence and resurgence of zoonotic infectious diseases. *Critical reviews in microbiology*, 33(4):243–299, 2007.

- [29] Cassandra Handan-Nader and Daniel E Ho. Deep learning to map concentrated animal feeding operations. *Nature Sustainability*, 2(4):298–306, 2019.
- [30] Galen Harrison, Przemyslaw Porebski, Jiangzhuo Chen, Mandy Wilson, Henning Mortveit, Parantapa Bhattacharya, Dawen Xie, Stefan Hoops, Anil Vullikanti, Li Xiong, et al. Synthetic information and digital twins for pandemic science: Challenges and opportunities. In *2023 5th IEEE International Conference on Trust, Privacy and Security in Intelligent Systems and Applications (TPS-ISA)*, pages 23–33. IEEE, 2023.
- [31] Stefan Hoops, Jiangzhuo Chen, Abhijin Adiga, Bryan Lewis, Henning Mortveit, Hannah Baek, Mandy Wilson, Dawen Xie, Samarth Swarup, Srinivasan Venkatramanan, et al. High Performance Agent-Based Modeling to Study Realistic Contact Tracing Protocols. In Kim Sojung, Ben Feng, Katy Smith, Sara Masoud, and Zeyu Zheng, editors, *2021 Winter Simulation Conference (WSC)*, pages 1–12. IEEE, 2021.
- [32] John M Humphreys, Andrew M Ramey, David C Douglas, Jennifer M Mullinax, Catherine Soos, Paul Link, Patrick Walther, and Diann J Prosser. Waterfowl occurrence and residence time as indicators of h5 and h7 avian influenza in north american poultry. *Scientific Reports*, 10(1):2592, 2020.
- [33] Cliff C Kerr, Robyn M Stuart, Dina Mistry, Romesh G Abeysuriya, Katherine Rosenfeld, Gregory R Hart, Rafael C Núñez, Jamie A Cohen, Prashanth Selvaraj, Brittany Hagedorn, et al. Covasim: An Agent-Based Model of COVID-19 Dynamics and Interventions. *PLOS Computational Biology*, 17(7):e1009149, 2021.
- [34] A Marm Kilpatrick, Aleksei A Chmura, David W Gibbons, Robert C Fleischer, Peter P Marra, and Peter Daszak. Predicting the global spread of H5N1 avian influenza. *Proceedings of the National Academy of Sciences*, 103(51):19368–19373, 2006.
- [35] Mariana Leguia, Alejandra Garcia-Glaessner, Breno Muñoz-Saavedra, Diana Juarez, Patricia Barrera, Carlos Calvo-Mac, Javier Jara, Walter Silva, Karl Ploog, Lady Amaro, et al. Highly pathogenic avian influenza A (H5N1) in marine mammals and seabirds in Peru. *Nature Communications*, 14(1):5489, 2023.
- [36] Yuying Liang. Pathogenicity and virulence of influenza. *Virulence*, 14(1):2223057, 2023.
- [37] Kacper Libera, Kacper Konieczny, Julia Grabska, Wiktoria Szopka, Agata Augustyniak, and Małgorzata Pomorska-Mól. Selected livestock-associated zoonoses as a growing challenge for public health. *Infectious disease reports*, 14(1):63–81, 2022.
- [38] Hinh Ly. Highly pathogenic avian influenza H5N1 virus infections of dairy cattle and livestock handlers in the United States of America, 2024.
- [39] James M MacDonald and William D McBride. The transformation of us livestock agriculture scale, efficiency, and risks. Economic Information Bulletin No. 43, Economic Research Service, U.S. Dept. of Agriculture, 2009.
- [40] Madhav V Marathe, Henning S Mortveit, Nidhi Parikh, and Samarth Swarup. Prescriptive analytics using synthetic information. In *Emerging Methods in Predictive Analytics: Risk Management and Decision-Making*, pages 1–19. IGI Global, 2014.
- [41] Rounak Meyur, Anil Vullikanti, Samarth Swarup, Henning S Mortveit, Virgilio Centeno, Arun Phadke, H Vincent Poor, and Madhav V Marathe. Ensembles of realistic power distribution networks. *Proceedings of the National Academy of Sciences*, 119(42):e2205772119, 2022.
- [42] Mark H Myer and John M Johnston. Spatiotemporal bayesian modeling of west nile virus: Identifying risk of infection in mosquitoes with local-scale predictors. *Science of the Total Environment*, 650:2818–2829, 2019.

- [43] USDA National Agricultural Statistics Service. Census of Agriculture. <https://www.nass.usda.gov/AgCensus/>. [Accessed 03-Jan-2023].
- [44] USDA National Agricultural Statistics Service. Census of Agriculture. <https://www.nass.usda.gov/datasets/qs.census2022.txt.gz>. [Accessed 11-Jun-2024].
- [45] Thao-Quyen Nguyen, Carl Hutter, Alexey Markin, Megan N Thomas, Kristina Lantz, Mary Lea Killian, Garrett M Janzen, Sriram Vijendran, Sanket Wagle, Blake Inderski, et al. Emergence and interstate spread of highly pathogenic avian influenza a (h5n1) in dairy cattle. *bioRxiv*, pages 2024–05, 2024.
- [46] Colorado Department of Agriculture. HPAI in Dairy Cattle. <https://ag.colorado.gov/animal-health/reportable-diseases/avian-influenza/hpai-in-dairy-cattle>. [Accessed 10-13-2024].
- [47] The University of Iowa. CAFOs in the US. <https://cafomaps.org/>. [Accessed 08-19-2024].
- [48] Björn Olsen, Vincent J Munster, Anders Wallensten, Jonas Waldenström, Albert DME Osterhaus, and Ron AM Fouchier. Global patterns of influenza A virus in wild birds. *science*, 312(5772):384–388, 2006.
- [49] Francine C Paim, Andrew S Bowman, Lauren Miller, Brandi J Feehan, Douglas Marthaler, Linda J Saif, and Anastasia N Vlasova. Epidemiology of deltacoronaviruses (δ -cov) and gammacoronaviruses (γ -cov) in wild birds in the united states. *Viruses*, 11(10):897, 2019.
- [50] Kelly A Patyk, Mary J McCool-Eye, David D South, Christopher L Burdett, Susan A Maroney, Andrew Fox, Grace Kuiper, and Sheryl Magzamen. Modelling the domestic poultry population in the united states: A novel approach leveraging remote sensing and synthetic data methods. *Geospatial Health*, 15(2), 2020.
- [51] SRAP project. State CAFO guides. <https://sraproject.org/state-cafo-guides/>. [Accessed 10-22-2024].
- [52] Diann J Prosser, Cody M Kent, Jeffery D Sullivan, Kelly A Patyk, Mary-Jane McCool, Mia Kim Torchetti, Kristina Lantz, and Jennifer M Mullinax. Using an adaptive modeling framework to identify avian influenza spillover risk at the wild-domestic interface. *Scientific Reports*, 14(1):14199, 2024.
- [53] Wendy Puryear, Kaitlin Sawatzki, Nichola Hill, Alexa Foss, Jonathon J Stone, Lynda Doughty, Dominique Walk, Katie Gilbert, Maureen Murray, Elena Cox, et al. Highly pathogenic avian influenza A (H5N1) virus outbreak in New England seals, United States. *Emerging Infectious Diseases*, 29(4):786, 2023.
- [54] Caleb Robinson, Ben Chugg, Brandon Anderson, Juan M Lavista Ferres, and Daniel E Ho. Mapping industrial poultry operations at scale with deep learning and aerial imagery. *IEEE Journal of Selected Topics in Applied Earth Observations and Remote Sensing*, 15:7458–7471, 2022.
- [55] Timothy P Robinson, GR William Wint, Giulia Conchedda, Thomas P Van Boeckel, Valentina Ercoli, Elisa Palamara, Giuseppina Cinardi, Laura D’Aietti, Simon I Hay, and Marius Gilbert. Mapping the global distribution of livestock. *PloS one*, 9(5):e96084, 2014.
- [56] Brian L Sullivan, Christopher L Wood, Marshall J Iliff, Rick E Bonney, Daniel Fink, and Steve Kelling. eBird: A citizen-based bird observation network in the biological sciences. *Biological conservation*, 142(10):2282–2292, 2009.
- [57] Christine M Szablewski, Chelsea Iwamoto, Sonja J Olsen, Carolyn M Greene, Lindsey M Duca, C Todd Davis, Kira C Coggeshall, William W Davis, Gideon O Emukule, Philip L Gould, et al. Reported global avian influenza detections among humans and animals during 2013-2022: comprehensive review and analysis of available surveillance data. *JMIR Public Health and Surveillance*, 9(1):e46383, 2023.

- [58] Swapna Thorve, Young Yun Baek, Samarth Swarup, Henning Mortveit, Achla Marathe, Anil Vullikanti, and Madhav Marathe. High resolution synthetic residential energy use profiles for the United States. *Scientific Data*, 10(1):76, 2023.
- [59] Marcela M Uhart, Ralph ET Vanstreels, Martha I Nelson, Valeria Olivera, Julieta Campagna, Victoria Zavattieri, Philippe Lemey, Claudio Campagna, Valeria Falabella, and Agustina Rimondi. Massive outbreak of Influenza A H5N1 in elephant seals at Peninsula Valdes, Argentina: increased evidence for mammal-to-mammal transmission. *bioRxiv*, pages 2024–05, 2024.
- [60] Mary van Andel, Michael J Tildesley, and M Carolyn Gates. Challenges and opportunities for using national animal datasets to support foot-and-mouth disease control. *Transboundary and Emerging Diseases*, 68(4):1800–1813, 2021.
- [61] Yanni Xiao, Damian Clancy, Nigel P French, and Roger G Bowers. A semi-stochastic model for salmonella infection in a multi-group herd. *Mathematical Biosciences*, 200(2):214–233, 2006.
- [62] Rui Yuan, S Ali Pourmousavi, Wen L Soong, Andrew J Black, Jon AR Liisberg, and Julian Lemos-Vinasco. A synthetic dataset of Danish residential electricity prosumers. *Scientific Data*, 10(1):371, 2023.
- [63] Chuanyong Zhu, Renqiang Li, Mengyi Qiu, Changtong Zhu, Yichao Gai, Ling Li, Na Yang, Lei Sun, Chen Wang, Baolin Wang, et al. High spatiotemporal resolution ammonia emission inventory from typical industrial and agricultural province of China from 2000 to 2020. *Science of The Total Environment*, 918:170732, 2024.

6 Acknowledgements

We thank members of the Biocomplexity Institute and UVA Research computing for their support. We also thank VA PGCOE members, members of the Office for Pandemic Preparedness and Response Policy, Dan Hanfling, and Cyrus Shahpur, members of the National Security Council, Shankar Sundaram and Rachel Idowu, and CDC staff members, Eleanor Click and John Barnes for their thoughtful comments and suggestions. This work was partially supported by University of Virginia Strategic Investment Fund award number SIF160, National Science Foundation (NSF) Expeditions in Computing Grant CCF-1918656, PGCoE CDC-RFA-CK22-2204, DTRA subcontract/ARA S-D00189-15-TO-01-UVA, USDA-NIFA and NSF under the AI Institute: Agricultural AI for Transforming Workforce and Decision Support (AgAID) award No. 2021-67021-35344, USDA-NIFA under the Network Models of Food Systems and their Application to Invasive Species Spread, grant no. 2019-67021-29933. Any opinions, findings, conclusions, or recommendations expressed in this publication are those of the authors and do not necessarily reflect the views of the funding agencies. Its contents are solely the responsibility of the authors and do not necessarily represent the official views of the Centers for Disease Control and Prevention.

Supplementary Information

A Livestock

A.1 Organization and Preliminary Definitions

The types of livestock covered in this work are shown in Table 2. Two data sources were used to construct the livestock layers: Census of Agriculture (AGCENSUS) and Gridded Livestock of the World (GLW). These are described in the following sections. The overview of the methodology used to fill gaps, generate farms, and assigning them to grid cells is captured in Figure 6. The description of the same appears in Sections A.4 and A.6.

A **livestock type** refers to a class of animals. Examples of livestock type include cattle, poultry, hog, and sheep. A **livestock subtype** represents a subclass of animals within a livestock type. For example, the livestock type cattle includes subtypes such as beef cows and milk cows. Likewise, the livestock type poultry includes subtypes such as (egg) layers, pullets, turkeys, etc.

A.2 Census of Agriculture AgCensus

A.2.1 Data organization and availability

AGCENSUS provides counts of heads (i.e., population size) and farms for various livestock types and subtypes. The data is available at three different administrative levels – country, state, and county. The livestock types we consider here are cattle, poultry, hogs, and sheep. We also consider various subtypes for cattle and poultry. These are summarized in Table 2. The data organization is livestock type specific, making it a non-trivial task to extract relevant information. For each administrative level, the total counts are provided. Also provided are counts corresponding to different farm sizes. Farms are binned into categories based on the head counts of the corresponding livestock type, such as 1–24, 25–49, 50–99, 100–199, 200–499, 500–999, and 1000 or more, where each category is specified by the minimum and maximum head count, respectively, in the member farm. Accordingly, we have four types of counts: (i) state-total, (ii) state-by-farm-size, (iii) county-total, and (iv) county-by-farm-size. Table 3 depicts this organization of counts at the county level. The set of farm categories for each subtype is consistent with that of its parent livestock type.

Missing data. In many instances, head counts are redacted. The more refined the count category, the greater the incidence of missing data. There are more instances of missing data (i) at the county level compared to state level, (ii) in the farm-size categories compared to total head counts, and (iii) in subtype counts compared to total livestock counts. This can be observed in Table 2 for head counts aggregated using different types of counts. Operation counts, on the other hand, are always provided. For all livestock types except poultry, farm counts are provided at every administrative level for every farm category.

Notation. We set up some formal notation here to facilitate the description of our framework. Since each livestock type is processed independently, the notation will not carry information about the livestock type; it is assumed that the livestock type is known. The same holds true for the administrative level. Given a livestock type, the number of categories is denoted by ℓ . Then, for $i = 1, \dots, \ell$, a category is specified by (W_i^{\min}, W_i^{\max}) , the minimum and maximum population sizes respectively. Given an administrative level, let H denote the total head count and F denote the total farm count. For farm category i , let H_i and F_i denote the head and farm counts, respectively. Let Γ denote the set of different subtypes. The notation is similar to the one developed above; for a subtype $\gamma \in \Gamma$, H_γ and F_γ denote the total counts of the subtype at the target administrative level, and $H_{\gamma k}$ and $F_{\gamma k}$ denote the farm category specific counts for category $k = 1, \dots, \ell$.

Table 2: Population and operations statistics for various livestock types covered by our synthetic dataset. Also shown are the counts after filling gaps.

livestock	subtype	heads			final	farms	
		state tot.	county tot.	filled gaps		state	processed
cattle	all	87,954,742	85,973,763	85,973,763	87,932,032	732,123	731,981
	beef	29,214,479	27,790,671	29,207,376	29,199,243	622,162	622,050
	milk	9,309,855	7,526,842	9,317,802	9,317,612	36,024	35,996
	other	49,430,408	46,255,380	49,422,350	49,415,177	594,222	594,108
hogs	all	73,645,928	62,541,219	73,810,004	73,808,393	60,809	60,731
poultry	chukars	1,036,946	621,024	1,048,787	1,047,104	801	800
	ckn-broilers	1,737,674,957	1,680,674,087	1,737,674,725	1,737,795,431	42,991	42,947
	ckn-layers	375,927,945	199,001,866	388,508,984	389,641,754	24,0530	24,0270
	ckn-pullets	139,203,843	82,678,506	144,030,350	144,029,544	34,874	34,829
	ckn-roosters	7,656,478	6,858,454	7,720,552	7,720,400	42,110	42,064
	ducks	4,341,317	3,422,540	4,448,858	4,448,287	34,781	34,724
	emus	12,538	9,462	12,440	12,427	1,566	1,561
	geese	101,823	83,174	101,521	101,320	11,940	11,911
	guineas	391,931	340,504	391,674	391,549	18,853	18,844
	ostriches	2,245	1,519	3,496	3,496	232	232
	partridges	49,162	9,462	61,147	61,147	68	68
	peafowl	54,947	42,795	54,679	54,669	6,930	6,928
	pheasants	3,187,136	1,243,764	3,279,830	3,266,790	2,257	2,255
	pigeons	212,559	160,312	302,934	285,600	2,196	2,194
	poultry-other	69,840	37,923	84,241	84,241	789	789
	quail	9,188,443	6,245,272	9,294,150	9,293,769	4,738	4,731
	rheas	1,013	382	1,122	1,122	152	152
	turkeys	97,064,430	84,529,090	97,312,274	97,311,591	23,431	23,373
sheep	all	5,104,328	3,664,088	5,103,716	5,102,574	88,853	88,795

A.2.2 Livestock type-specific information

The relevant head and farm counts were extracted from the full AgCensus dataset by querying out the rows where `statisticcat_desc="INVENTORY"`; these rows are further filtered by `unit_desc="HEAD"` or `unit_desc="OPERATIONS"`, depending on whether head counts or number of operations are being calculated, respectively. The state- and county-level counts were extracted by filtering `agg_level` to `STATE` and `COUNTY`, respectively.

Cattle. The counts were obtained by extracting rows where `commodity_desc="CATTLE"`. The cattle population is categorized into three subtypes, `beef`, `milk`, and `other` (specified by the `class_desc` field). The total count of cattle was obtained by setting `class_desc="INCL CALVES"`. The state- and county-total counts were obtained by extracting rows where `domain_desc="TOTAL"`. The state-by-farm-size and county-by-farm-size counts were obtained by setting `domain_desc≠"TOTAL"`. There are several additional conditions that had to be filtered to get the appropriate counts. These conditions only include rows where (i) `domaincat_desc` text includes text "0 HEAD" or "1 OR MORE HEAD"; (ii) (`domain_desc` includes text such as "inventory of milk/beef cows" or "inventory of cows" and (iii) `class_desc` is either "INCL CALVES" or "EXCL COWS").

Table 3: The data format for state-by-farm-size and county-by-farm-size. Some of the head counts data is redacted. The corresponding totals (either state or county) are denoted by H (for “all”), H_{beef} , H_{milk} and H_{other} . Depending on the instance, any of the totals or counts by farm-size can be missing.

Cat.	Farm size	all	beef	milk	other
1	1–9	(F_1, H_1)	$(F_{1,\text{beef}}, H_{1,\text{beef}})$	$(F_{1,\text{milk}}, H_{1,\text{milk}})$	$(F_{1,\text{other}}, H_{1,\text{other}})$
2	10–19	(F_2, H_2)	$(F_{2,\text{beef}}, H_{2,\text{beef}})$	$(F_{2,\text{milk}}, H_{2,\text{milk}})$	$(F_{2,\text{other}}, H_{2,\text{other}})$
	\vdots			\dots	
i	$W_i^{\min} - W_i^{\max}$	(F_i, H_i)	$(F_{i,\text{beef}}, H_{i,\text{beef}})$	$(F_{i,\text{milk}}, H_{i,\text{milk}})$	$(F_{i,\text{other}}, H_{i,\text{other}})$
	\vdots			\dots	

Poultry. Poultry data has many subtypes. In AGCENSUS each subtype is organized as separate livestock under the group poultry, i.e., `group_desc="POULTRY"`. We remapped this data by creating a new livestock called `poultry` and mapping all livestock under it to distinct subtypes. The counts for chickens were obtained by setting `commodity_desc="CHICKENS"`. There are four subtypes corresponding to chickens: layers (`ckn-layers`), broilers (`ckn-broilers`), pullets (`ckn-pullets`), and roosters (`ckn-roosters`). For layers, state-level counts of farms by category is present. However, we have ignored this as the corresponding head counts are absent. The counts of other poultry such as turkeys and ducks was obtained by setting `group_desc="POULTRY"` and `commodity_desc ≠ "CHICKENS"`.

Hogs. The counts were obtained by setting `commodity_desc="HOGS"`. The rest are similar to cattle.

Sheep. The counts were obtained by setting `commodity_desc="SHEEP"` and `class=incl lambs`. No subtypes were considered. The remaining details are similar to cattle.

Aligning farm categories. Farm category specifications are more refined at the state level than at the county level. For example, at the county level, the largest category is 500 or more, whereas at the state level, there are categories such as 1000-2499 and 2500 or more. We mapped all state-level categories to county-level categories by either aggregating the counts in the additional categories or by simply removing the categories if they had already been accounted for at the county level.

A.3 Gridded Livestock of the World

The Gridded Livestock of the World [21] dataset provides a gridded distribution of livestock abundance at 5 arc minute resolution. The gridded distribution data was constructed by combining detailed livestock census statistics mined from various sources with random forest models with predictors of the following types: land use, human population, travel times, vegetation, and climate. Unsuitable areas such as water bodies and core urban centers are identified using land cover and human population density information. More details are provided in Gilbert et al. [27].

The data is available in the following format. Each grid cell is identified by a cell ID denoted by a pair of integers, (x, y) . For each grid cell, if a livestock abundance is available, the livestock type and value are provided. Among the livestock types or species provided, we considered cattle, buffaloes, sheep, pigs, chickens, and ducks. Buffaloes were mapped to cattle, and ducks and chickens were mapped to poultry. We did not consider goats and horses. No information on livestock subtypes is provided.

We identified the cells corresponding to the conterminus US and associated them with their respective state and county FIPS codes. The cells are denoted by C_j while the abundance value of a livestock type is denoted by Q_j . The notation does not include livestock type as each type is processed independently.

A.4 Filling gaps

As mentioned above, some head counts are missing in all count types: state-total, state-by-farmsize, county-total, and county-by-farm-size. We use a combination of integer linear programs (ILPs) and iterative proportional fitting (IPF) following Burdett et al. [8]. For cattle and poultry, gaps are filled for each subtype, while for hogs and sheep, they are filled for the livestock type.

We use the integer program Algorithm 1 to fill missing data for the following types of counts: state-total, state-by-farm-size, and county-total. It takes as input all the known counts, sum of all the counts, and bounds on the unknown counts and distributes equitably the heads that are unaccounted for to all entities for which the counts are missing. It respects the bounds provided as input.

Algorithm 1: FILLGAPS integer program to fill missing gaps in state and county totals and state counts by farm-size.

Input: No. of unknown quantities m , their sum total T , and bounds $((L_1, U_1), (L_2, U_2), \dots, (L_m, U_m))$, where $L_i \leq U_i$, $1 \leq i \leq m$.

Output: Assignment of values to the m unknown quantities. (The constraints to be satisfied by the unknown quantities are provided below.)

```

1 Variables
2  $x_i, i = 1, \dots, m$  // Variables for unknown quantities
3  $\lambda_0 \geq 0$  // Variable for equitable distribution

4 Constraints
5  $L_i \leq x_i \leq U_i, 1 \leq i \leq m$  // Bounds on unknown quantities based on input data
6  $\sum_i x_i = T$  // Sum of unknown quantities should be T
7  $x_i - L_i \leq \lambda_0$  // Bound the difference between the assigned quantities and
   corresponding lower bounds

8 Set Objective: Minimize  $\lambda_0$ 

9 return  $(x_1, x_2, \dots, x_m)$ 
```

Now, we describe the process used to fill missing data for each count type in the order in which they are processed.

1. **State-total head counts.** The total head count here corresponds to country head count which is available for every livestock subtype. There are potentially four sources that can be used to derive bounds. If farm counts per farm-size category are given at the state level, an initial set of lower and upper bounds can be derived as follows: $W_i^{\min} F_{i\gamma} \leq H_{i\gamma} \leq W_i^{\max} F_{i\gamma}$. The lower bounds are refined by using the available head counts for each farm size category. Similar refinement can be done from counts per farm size at the county level. The sum of the lower bounds across farm categories provides a lower bound for the state total. Finally, if county totals are provided for some counties of the state, their sum provides another lower bound. We set the final lower bound to be the maximum of bounds obtained as above. This data is fed to FILLGAPS to obtain estimates for the missing counts.
2. **State-by-farm-size head counts.** The total head count here corresponds to state total which is either available or estimated as above for every livestock subtype. We use the same approach as above by first deriving bounds based on number of farms in each category and then refining the lower bound using county-by-farm-size head counts. This data is fed to FILLGAPS to obtain estimates for the missing counts.
3. **County-total head counts.** The total head count here corresponds to the total head count in the state to which the county belongs, which is either available or estimated as above for every livestock subtype. If farm counts are provided for each farm category, then we use it to derive the initial bounds. This is further refined if county-by-farm-size head counts are provided. This data is fed to FILLGAPS to obtain estimates for the missing counts.
4. **County-by-farm-size head counts using IPF.** To fill gaps in county-by-farm-size counts, we follow the methodology of Burdett et al. [8]. They apply IPF [18, 23] for the case of hogs to estimate these

counts. Here, we give an overview of the method and refer to Burdett et al. [8] for details. The processing is done per state and subtype. In the IPF process, the objective is to impute missing values in a given matrix given row and column totals. In this case, the data matrix consists of county-by-farm-size counts with counties as rows and farm size categories as columns. Note that, at this stage, both county totals and state-by-farm-size counts are available either from data or by estimation. Unknown values in the matrix are seeded with the product of the average size of the corresponding category and the number of farms in that category.

A.5 Generation of farms

Objective. We are given farm categories $i = 1, \dots, \ell$. Let F_i and H_i denote the number of farms and livestock heads in category i . For $k = 1, \dots, \ell$, let $F_{\gamma k}$ and $H_{\gamma k}$ denote the number of farms and heads corresponding to category k with respect to subtype γ (see Table 3). The objective is to find an assignment of farms whose farm counts and composition respects these counts. Note that the categories are pairwise disjoint and cover the entire range. In addition to head counts of subtypes, we are also given counts of the livestock type as well by farm size. Since the IPF procedure does not account for these counts, there could be differences between this data and the counts obtained by aggregating farm subtype counts in our assignment. Our optimization objective is a linear combination of many parameters as discussed below.

- (a) To choose an assignment with minimum discrepancy with respect to known counts, we introduce a parameter λ_1 .
- (b) The parameter λ_2 in the minimization objective represents the largest number of subtypes in a farm.
- (c) The minimization objective includes ℓ parameters, denoted by λ_{3i} , $1 \leq i \leq \ell$. The purpose of parameter λ_{3i} is to ensure that the population of all the subtypes in any farm of category i is close to the average value for that farm category. The purpose of minimizing these parameters is to obtain an equitable distribution of the population across all farm categories.
- (d) The parameter λ_4 in the minimization objective is used to ensure that the sum of the head counts of subtype γ over all the farms assigned category k is close to the given head count $H_{\gamma k}$.

The optimization objective combines the above parameters into a linear function using appropriate scaling constants. These scaling constants ensure that parameters with larger values have larger penalties. As a consequence, the solver will aggressively minimize parameters with larger values compared to ones with smaller values.

Algorithm 2: GENFARMS. Integer linear program to generate farms consistent with input counts of farms and head counts.

Input: County-by-farm-size head and farm counts as in Table 3.

Output: Farms with head counts of each subtype.

```

1 Variables
2 For each farm  $f$  in category  $i$ ,  $h_{if\gamma}$  corresponds to the population of subtype  $\gamma$  in that farm;
3 For each farm  $f$  in category  $i$ ,  $x_{if\gamma k}$  indicates whether  $(f, i)$  belongs to category  $k$  w.r.t. subtype  $\gamma$ ;
4 For each farm  $f$  in category  $i$ ,  $y_{if\gamma k}$  indicates whether  $h_{if\gamma} = 0$ ;
5 For each farm  $f$  in category  $i$ ,  $z_{if\gamma k} = h_{if\gamma}$  if  $h_{if\gamma}$  belongs to the category  $k$  with respect to
   subtype  $\gamma$ . Otherwise, it is 0.
6 Variables for minimization objectives:  $\lambda_1$  (alignment with known total population within each farm
   size category),  $\lambda_2$  (minimize number of subtypes per farm),  $\lambda_{3i}$ ,  $i \in [1, \ell]$  (equitable distribution of
   population in each farm size category), and (alignment with subtype population within each farm
   size category)  $\lambda_4$ .

7 Constraints
8 Let  $M$  be a suitably large constant;
   // Population and farm size constraints
9  $W_i^{\min} \leq \sum_{\gamma} h_{if\gamma} \leq W_i^{\max}$  // Category farm size constraint

   // Subtype farm category constraints: Farm counts.
10  $i \in [1, \ell], f \in [1, F_i], \gamma \in \Gamma, k \in [1, \ell], h_{if\gamma} \geq W_k^{\min} - (1 - x_{if\gamma k}) \cdot M$  // Lower bound
11  $i \in [1, \ell], f \in [1, F_i], \gamma \in \Gamma, k \in [1, \ell], h_{if\gamma} \leq W_k^{\max} + (1 - x_{if\gamma k}) \cdot M$  // Upper bound
12  $i \in [1, \ell], f \in [1, F_i], \gamma \in \Gamma, k \in [1, \ell], h_{if\gamma} \geq 1 - y_{if\gamma k}$  // Lower bound when subtype count is 0
13  $i \in [1, \ell], f \in [1, F_i], \gamma \in \Gamma, k \in [1, \ell], h_{if\gamma} \leq (1 - y_{if\gamma k}) \cdot M$  // Upper bound when subtype count
   is 0
14  $i \in [1, \ell], f \in [1, F_i], \gamma \in \Gamma, \sum_k x_{if\gamma k} + y_{if\gamma k} = 1$  // Farm in exactly one category
15  $\gamma \in \Gamma, k = [1, \ell], \sum_{f,i} x_{if\gamma k} = F_{\gamma k}$  // Count equals total farms in that category

   // Subtype farm category constraints: Population counts
16  $i = [1, \ell], f = [1, F_i], \gamma \in \Gamma, k = [1, \ell], z_{if\gamma k} \leq h_{if\gamma}$  // Upper bound
17  $i = [1, \ell], f = [1, F_i], \gamma \in \Gamma, k = [1, \ell], z_{if\gamma k} \leq x_{if\gamma k} \cdot M$  //  $x_{if\gamma k} = 0 \Rightarrow z_{if\gamma k} = 0$ 
18  $i = [1, \ell], f = [1, F_i], \gamma \in \Gamma, k = [1, \ell], z_{if\gamma k} \geq h_{if\gamma} - (1 - x_{if\gamma k}) \cdot M$  //  $x_{if\gamma k} = 1 \Rightarrow z_{if\gamma k} = h_{if\gamma}$ 
19  $\gamma \in \Gamma, k = [1, \ell], \left| \sum_{f,i} z_{if\gamma k} - H_{\gamma k} \right| \leq \lambda_4$  // Count must be close to  $H_{\gamma k}$ 

   // The assignment should be such that it is as close a match to the total
   population distribution in each category,  $H_i$ .
20  $i = [1, \ell], \left| \sum_{f,\gamma} h_{if\gamma} - H_i \right| \leq \lambda_1$ .

   // Subtype distribution: Minimize number of subtypes per farm
21  $i = [1, \ell], f = [1, F_i], \sum_{\gamma,k} x_{if\gamma k} \leq \lambda_2$ 

   // Equitable distribution in each category.
22  $i = [1, \ell], a_i = \sum_{f,\gamma} h_{if\gamma} / F_i$ , // Average population in each farm category
23  $i = [1, \ell], f = [1, F_i], \left| \sum_{\gamma} h_{if\gamma} - a_i \right| \leq \lambda_{3i}$ 

24 Set objective. Minimize  $\lambda_1 + (H + 1) \cdot \lambda_2 + (|\Gamma| + 1)(H + 1) \cdot \sum_i \lambda_{3i} + (|\Gamma| + 1)(H + 1)^2 \cdot \lambda_4$ .
25 return  $(h_{if\gamma} \mid i = [1, \ell], f = [1, F_i], \gamma \in \Gamma)$ 

```

Implementation notes. The algorithm was run for each county–livestock instance in parallel on a HPC cluster. For faster convergence to a solution, we set the MIP gap (which refers to the percentage difference between the current best feasible solution and the best known bound on the optimal objective value) to 0.1%

of the total head count for each instance.

A.6 Farms to cells

Objective. We are given N_f farms with number of heads in each farm f_i denoted by P_i , $i = 1, \dots, N_f$, and N_c cells with number of heads in each cell C_j denoted by Q_j , $j = 1, \dots, N_c$. The objective is to assign to each farm f_i a cell C_j such that $\max_j |\sum_{i, \delta_i=j} P_i - Q_j|$ is minimized, where $\delta_i = j$ if and only if f_i is assigned cell C_j .

Algorithm 3: FARMSTOCeLLS. Integer linear program to generate farms consistent with input counts of farms and head counts.

Input: Farms f_i , $i = [1, N_f]$ with total head count P_i , cells C_j , $j = [1, N_c]$ with head count Q_j .

Output: Assignment of each farm to a cell.

1 Variables

- 2** For $1 \leq i \leq N_f$ and $1 \leq j \leq N_c$, x_{ij} indicates whether farm f_i is assigned to cell C_j : $x_{ij} = 1$ if f_i is assigned cell C_j ; otherwise, $x_{ij} = 0$;
- 3** For $1 \leq i \leq N_f$ and $1 \leq j \leq N_c$, $h_{ij} = P_i$ if $x_{ij} = 1$, else 0;
- 4** Let λ_4 be a positive integer variable that is equal to $\max_j |\sum_{i, \delta_i=j} P_i - Q_j|$;

5 Constraints

// Assign farm to a cell

- 6** $1 \leq i \leq N_f, 1 \leq j \leq N_c$, $h_{ij} = x_{ij} \cdot P_i$ // Contribution of a farm to cell population
- 7** $1 \leq i \leq N_f$, $\sum_j x_{ij} = 1$ // Each farm belongs to exactly one cell
- 8** $1 \leq j \leq N_c$, $|\sum_i h_{ij} - Q_j| \leq \lambda_5$ // Farm assignment should align with cell capacities

9 Set objective. Minimize λ_5 .

10 return ($h_{if\gamma} \mid i = [1, \ell], f = [1, F_i], \gamma \in \Gamma$)

Implementation notes. The algorithm was run for each county–livestock instance in parallel on a HPC cluster. For faster convergence to a solution, we set the MIP gap to 0.01% of the total head count for each instance.

B Wild Birds

Our processing pipeline to extract abundance data involves the following steps:

- **Coordinate System Conversion:** We transform the data from its original World Eckert IV equal-area projection (ESRI:54012) to a standard geographic coordinate system (EPSG:4326) to ensure compatibility with other geospatial datasets in our study.
- **Spatial Sampling:** To balance spatial resolution with computational efficiency, we sampled the data at regular intervals consistent with the GLW grid cell dimensions. This sampling strategy preserves the overall spatial patterns while reducing the dataset to a manageable size.
- **Temporal Resolution:** We maintained the weekly temporal resolution provided by eBird, allowing for detailed analysis of seasonal migration patterns.

C Additional Information on Processing Centers

The USDA [3] maintains a comprehensive list of approved dairy plants, including pasteurization facilities, which are inspected at least twice yearly. These inspections cover over 100 items, including milk supply, plant facilities, equipment condition, sanitary practices, and processing procedures. While most commercial dairy

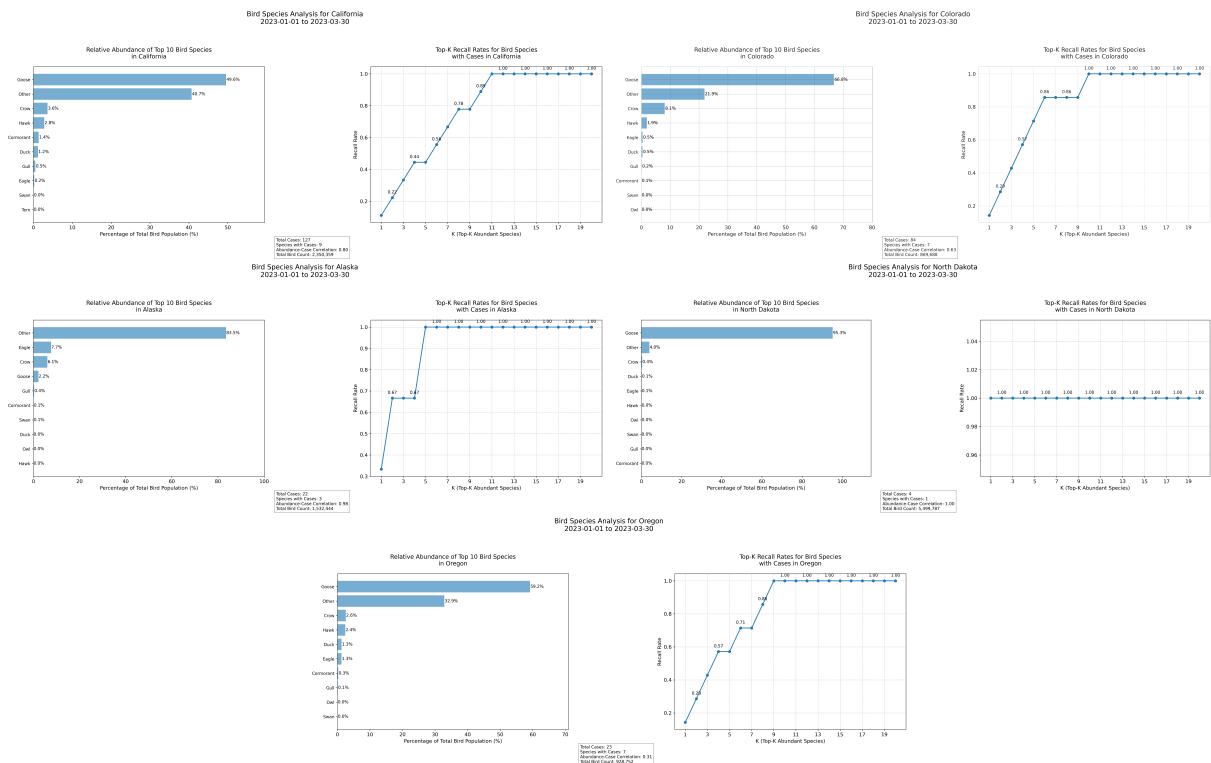


Figure 8: Bird Abundance and H5N1 incidence data from January to March 2023. new birds data

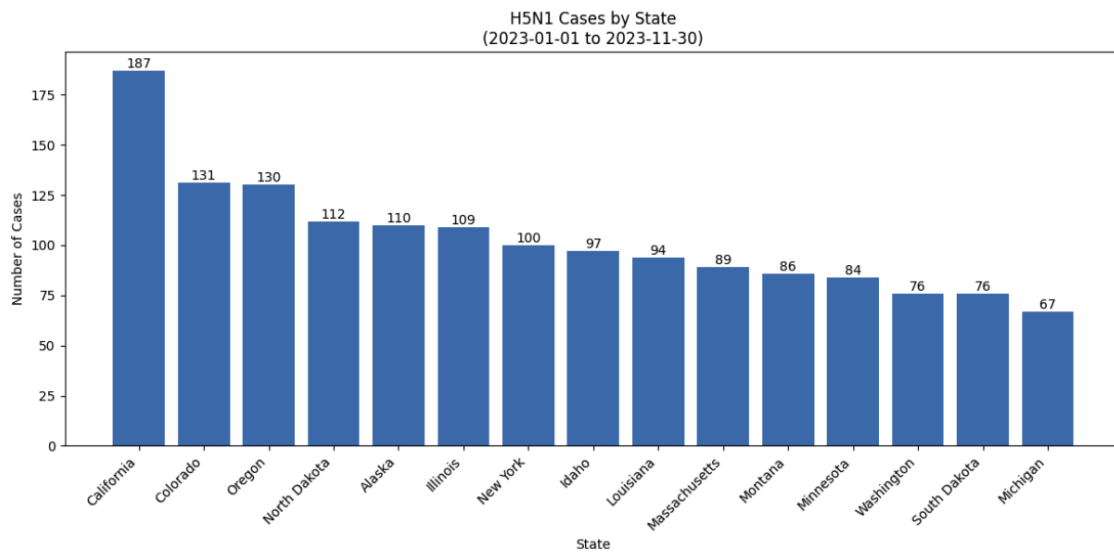


Figure 9: H5N1 incidence in wild birds across different states from 2022-2024. Total cases in period: 1,548 and Number of states affected: 48

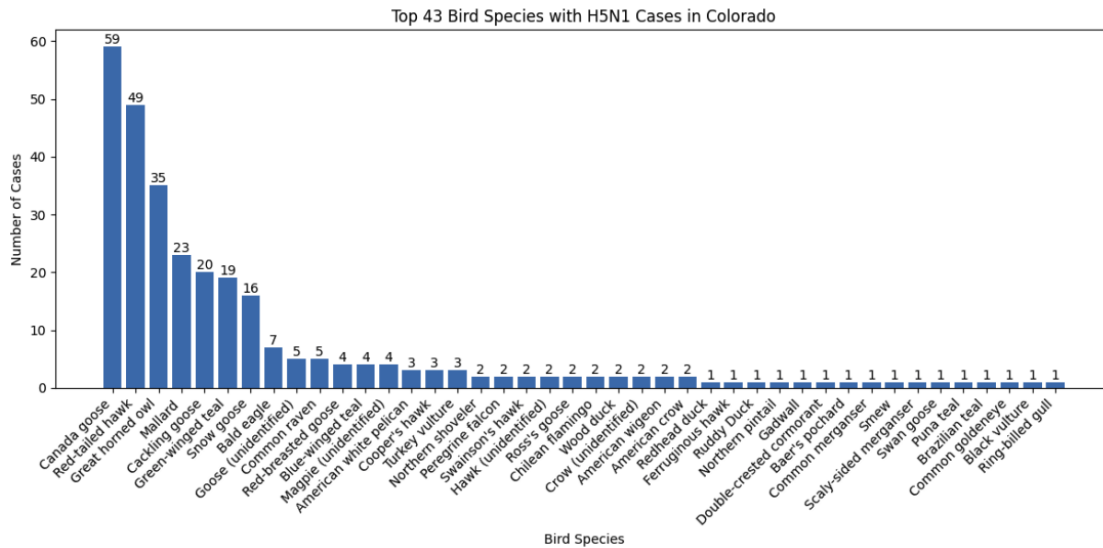


Figure 10: H5N1 incidence in wild birds across different species (total 43 species infected). We use abundance patterns for these species to conduct analysis and risk estimation

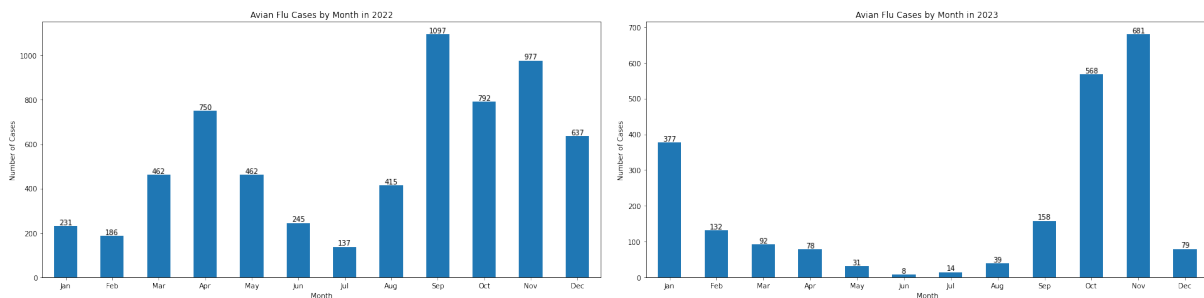


Figure 11: H5N1 incidence in wild birds across different months in 2022 and 2023. Case abundance is higher in fall and winter months, which can be attributed to breeding and migration patterns and viral transmissibility in colder months.

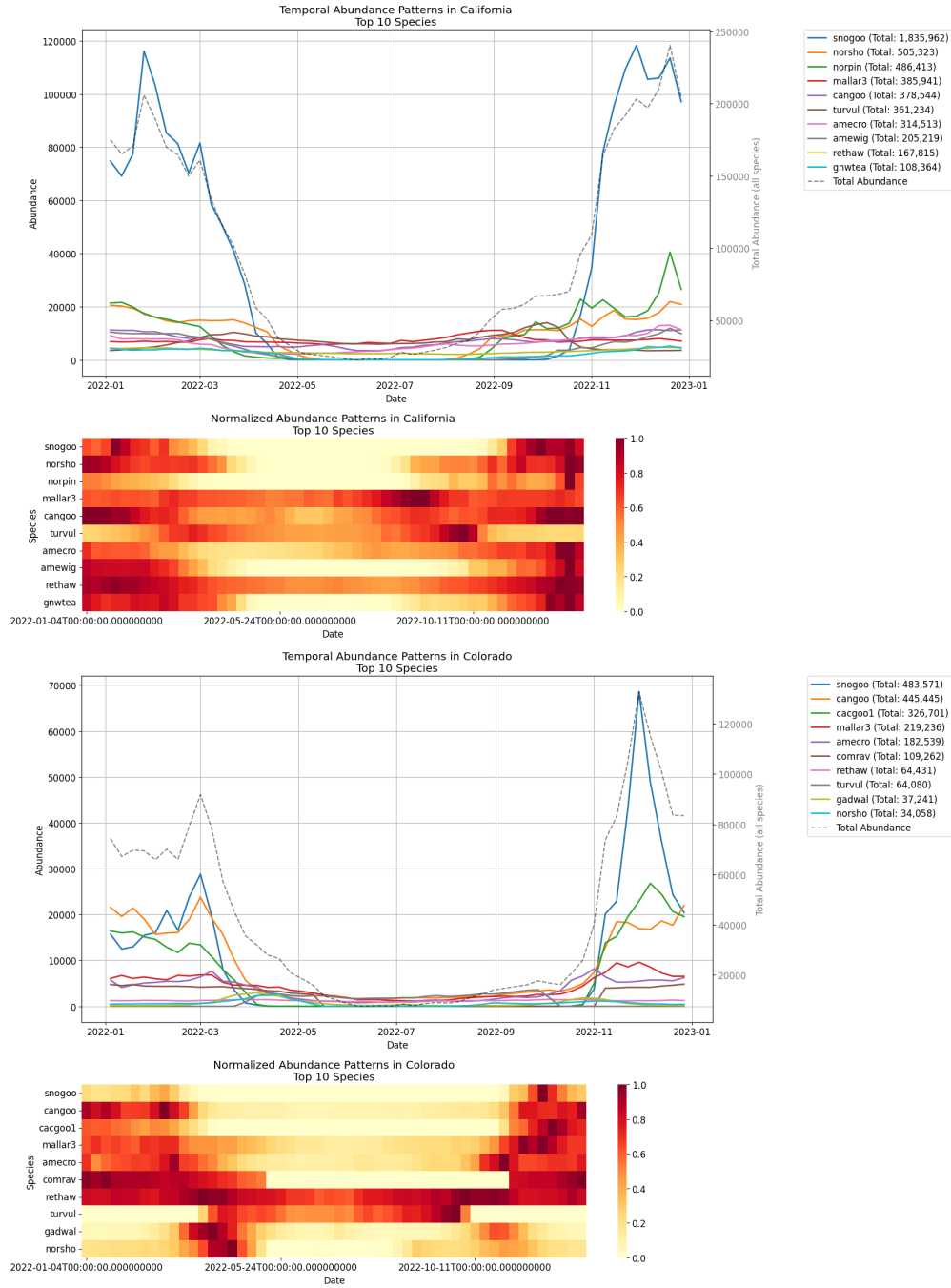


Figure 12: Temporal Abundance Pattern of Bird Species across states. We observe heterogeneity of species abundance and demographics across different states, throughout the year. Abundance varies across seasons due to migration and breeding in different geographies.

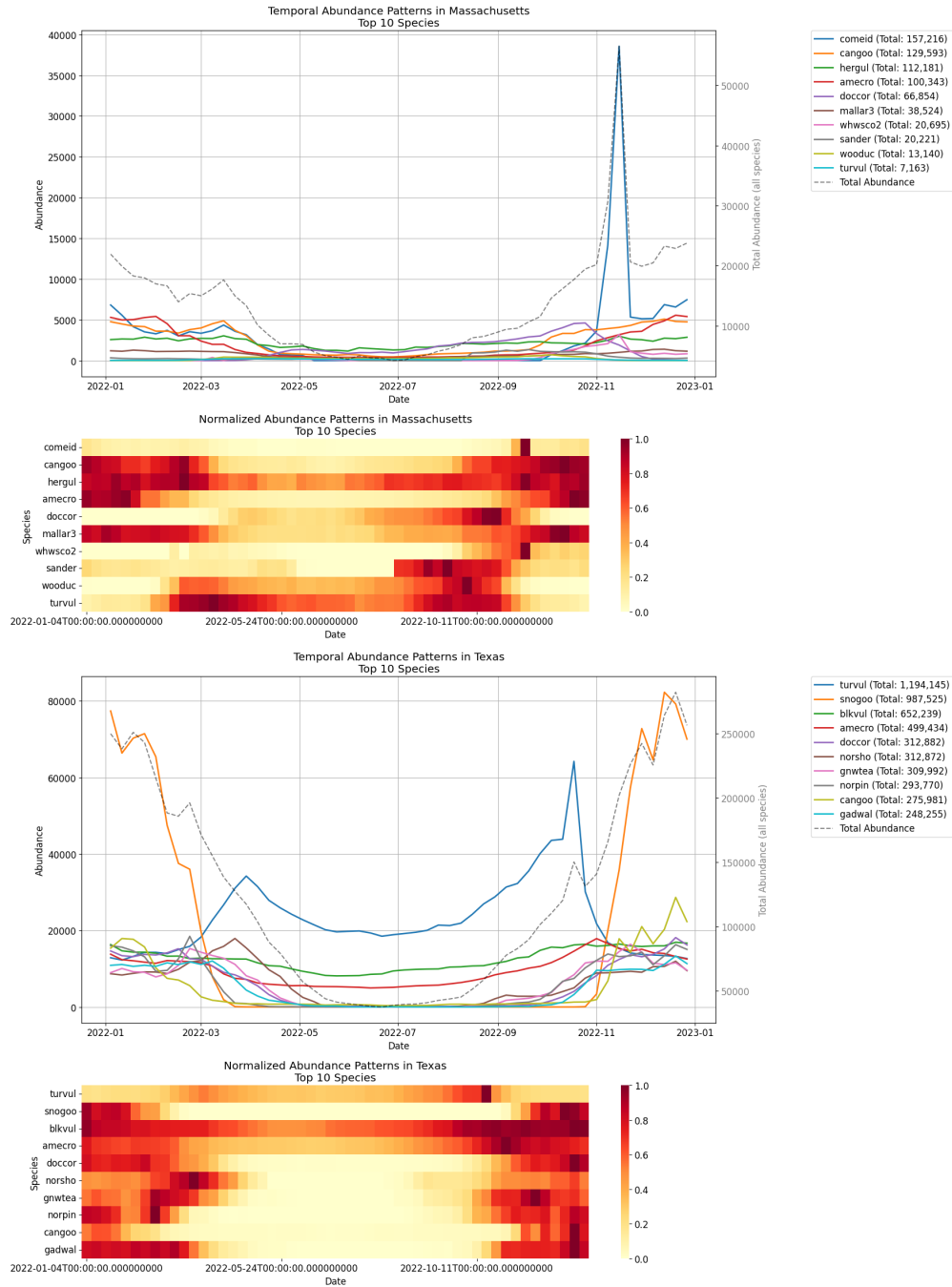


Figure 13: Temporal Abundance Pattern of Bird Species across states. We observe heterogeneity of species abundance and demographics across different states, throughout the year. Abundance varies across seasons due to migration and breeding in different geographies.

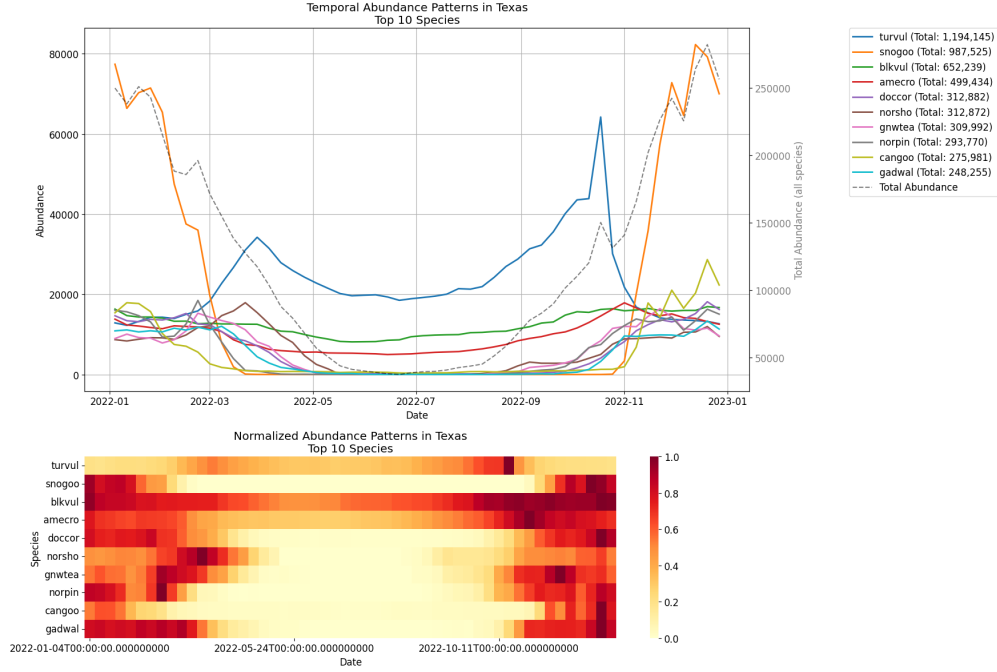


Figure 14: Temporal Abundance Pattern of Bird Species across states. We observe heterogeneity of species abundance and demographics across different states, throughout the year. Abundance varies across seasons due to migration and breeding in different geographies.

operations use pasteurized milk due to food safety regulations, some facilities may handle unpasteurized milk for specific products or processes.

The USDA assigns dairy plant approvals using two categories:

- Section I: Plants that produce products manufactured from dairy ingredients meeting USDA requirements or originating from USDA-approved plants. These are generally considered lower risk in terms of handling unpasteurized milk. (designated B, C, D, F, M, S and W codes)
- Section II: Plants that may have products produced from dairy ingredients that did not originate from USDA-approved plants (unapproved source plants). These plants potentially pose a higher risk of handling unpasteurized milk. (designated P codes)

We categorize product codes based on their potential risk of interaction with unpasteurized milk in Table 4.

Risk Level	Product Codes	Description
High Risk	M1, M2, M3, M6, M7, M8, M9	Raw milk, cream, and concentrated milk products
High Risk	C3-C47	Cheese types use unpasteurized milk
High Risk	B1-B9	Butter products, made from unpasteurized cream
Medium Risk	M10, M11, M12, M13, M14	Processed milk products involve some heat treatment
Low Risk	D1-D18	Dry milk products, undergo heat treatment during processing
Low Risk	W1-W25	Whey products, derived from pasteurized milk during cheese-making
Low Risk	F1-F15	Frozen dessert products, made with pasteurized ingredients
Low Risk	S4-S46	Specialty products, involve processing that would eliminate pathogens

Table 4: Risk of engaging with unpasteurized milk for different plant codes.